Petrology, Vol. 13, No. 4, 2005, pp. 352–380. Translated from Petrologiya, Vol. 13, No. 4, 2005, pp. 389–420.

Cenozoic Volcanism of Southeast Asia

P. I. Fedorov* and A. V. Koloskov**

**Geological Institute, Russian Academy of Sciences,*
Pyzhevskii per. 7, Moscow, 119017 Russia
e-mail: fedorov@ginras.ru
***Institute of Volcanology and Seismology, Far East Division,*
Russian Academy of Sciences, bul'v. Piipa 9, Petropavlovsk-Kamchatskii, 683006 Russia

Received May 20, 2004

Abstract—This paper presents an analysis of published and our own data on the geochemistry and isotopic systematics of the Cenozoic volcanic complexes of southeastern China, Vietnam, and Thailand and the adjoining East China and South China seas. Three large periods of volcanic activity were distinguished: Early Tertiary, Miocene, and Pliocene–Quaternary. The first period was characterized by the development of potassic basalt (absarokites and cocites in Vietnam) and tholeiitic bimodal (basalts and trachytes in southeastern China) volcanism, and the subsequent periods were dominated by intraplate-type tholeiitic and alkaline volcanism and minor occurrence of bimodal tholeiitic magmatism (basalts and rhyolites of the Okinawa Trough). The Cenozoic magmatic and geodynamic events were correlated over the region. It was shown that lateral and temporal variations in the compositions of the Miocene and Pliocene–Quaternary rocks reflect strong isotopic and geochemical heterogeneity of deep-seated magma sources.

INTRODUCTION

The India–Eurasia collision at 55–45 Ma (Khain, 2001) resulted in the movement of the Indochina, China, and Amur plates, which caused nappe formation and orogeny in the Tien Shan, displacements along the Red River, Three Pagodas, Wang Chao, Altyn Tagh, and Bolai fault zones (Tapponnier *et al.*, 1986), and rifting in the Baikal region (Rasskazov *et al.*, 2000). The collision disturbed the ternary junction of the Eurasian, Pacific, and Australian plates and was responsible for the opening of the Gulf of Thailand, the South China Sea, and the Andaman Sea (Le Pichon *et al.*, 1992) and formation of extensional structures in southern China and Indochina. Numerous volcanic areas associated with strike-slip and graben structures are mainly composed of basic rocks of the alkaline and tholeiitic series. Our new results on the Cenozoic volcanism of Vietnam and the South China Sea and the analysis of the available data on the southern China and Indochina regions allowed us to examine spatial and temporal variations in the chemistry of Cenozoic volcanics in this region, determine a general trend in their compositional evolution, and characterize their magma sources.

The chemical composition of rocks was investigated in the laboratories of the chemical analytical center of the Geological Institute, Russian Academy of Sciences. Major elements were determined by traditional wet chemical methods; Cr, Ni, and Co, by emission spectrometry (analyst I.Yu. Lubchenko); Rb, Ba, Sr, Y, and Nb, by the X-ray fluorescence method; Hf, Ta, Th, Sc, and rare earth element (REE), by instrumental neutron activation analysis (supervised by S.M. Lyapunov). Isotopic investigations were performed at Oregon State University, USA (analyst J. Davidson).

CENOZOIC VOLCANISM OF SOUTHEASTERN CHINA

The occurrences of Cenozoic volcanism in southeastern China (Figs. 1, 2) are mainly confined to northeast-trending rift systems, except for some areas related to the Red River shear zone. There were three major periods of volcanic activity: Early Tertiary, Miocene, and Pliocene–Quaternary.

The occurrences of Early Tertiary volcanism are restricted to the Guangdong and Yunnan provinces (Haidong region). The volcanism of the Guangdong province is confined to the Sanshui, Heyuan, and Lienping rift basins (Fig. 1; Chung *et al.*, 1997), which were probably initiated during the previous Late Mesozoic stage of rifting in China (Milanovskii and Nikishin, 1988). The late Paleocene–early Eocene tholeiites and trachytes of the Sanshui area compose a bimodal association (Table 1). The tholeiites show moderate concentrations of high field strength elements (HFSE) (Fig. 3b) and low La_n/Yb_n ratios (4.0–5.9). In the Th–Hf–Ta diagram, the tholeiites occur in the E-MORB field near the boundary with WPB (Fig. 4a). Their $^{143}Nd/^{144}Nd$ ratios are not high (0.51268–0.51290) and close to those of E-MORB, whereas the $^{87}Sr/^{86}Sr$ values are elevated (0.70373–0.70625). The trachytes show extremely high $^{87}Sr/^{86}Sr$ ratios (0.70863–0.71266) in combination with $^{143}Nd/^{144}Nd$ values similar to those of the basalts (Fig. 5a), which suggests a considerable contribution of an upper crustal component to trachyte

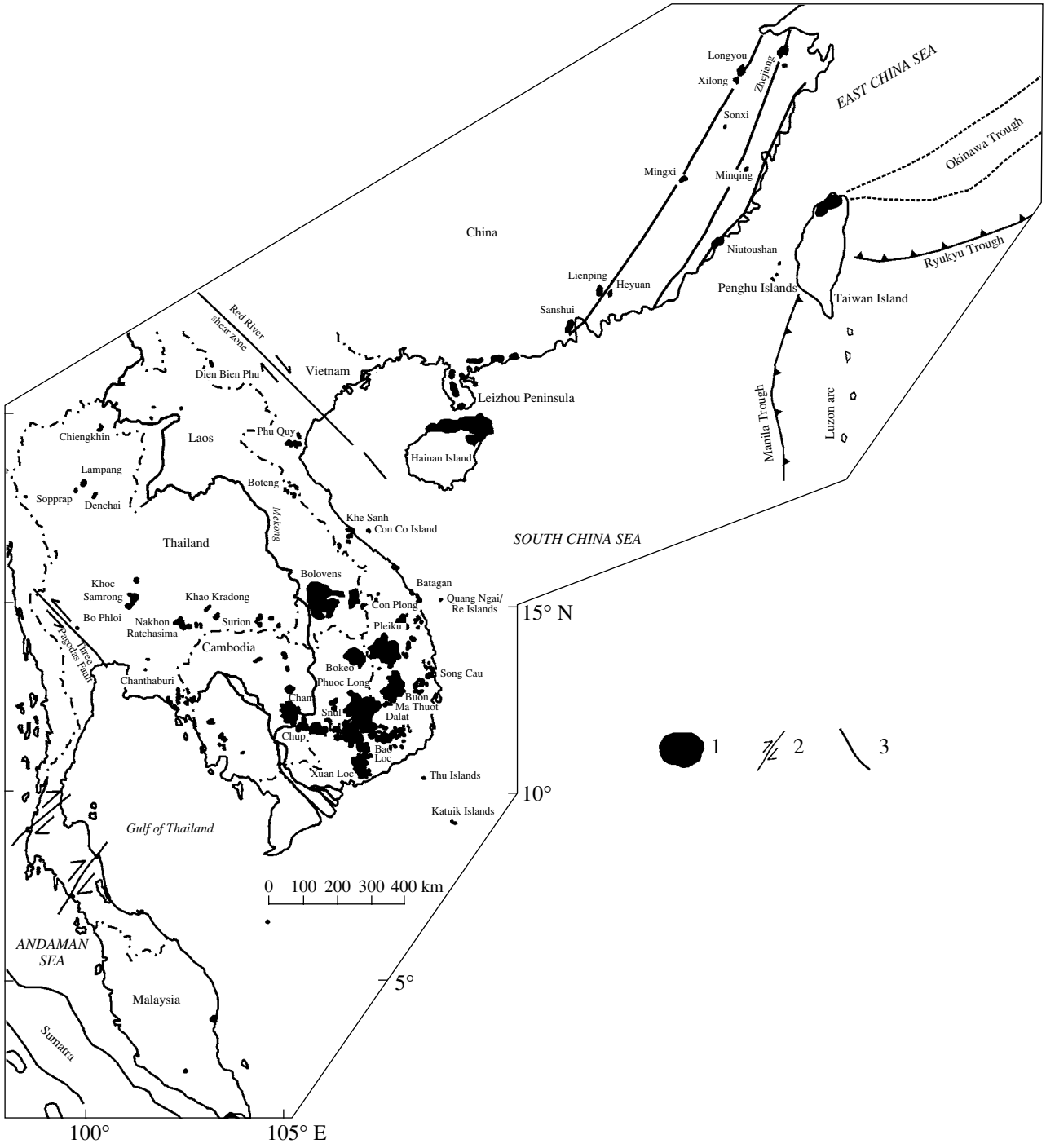

Fig. 1. Distribution of Cenozoic volcanic occurrences in Southeast Asia [modified after Barr and Macdonald (1981) and Whitford-Stark (1987)]. (1) Volcanic area, (2) strike-slip fault, and (3) other faults.

genesis. The basaltic andesites and andesites of the Heyuan area have less enriched compositions (La_n/Yb_n = 3.3–4.9); their $^{87}Sr/^{86}Sr$ ratios are similar to those of the Sanshui tholeiites and $^{143}Nd/^{144}Nd$ are lower (0.51258–0.51262). The basaltic andesites and andesites of the Lienping area are more LREE enriched (La_n/Yb_n = 8.1–12.9) and show a pronounced Ta–Nb minimum (Fig. 3b), high $^{87}Sr/^{86}Sr$ (0.70736–0.7109), and low $^{143}Nd/^{144}Nd$ (0.51232–0.51244). In the Th–Hf–Ta diagram (Fig. 4a), the volcanics plot within the IAB field. The potassic mafic volcanics of the Haidong area (30–40 Ma) are characterized by low HFSE and high large ion lithophile element (LILE) concentrations, a Ta–Nb minimum (Fig. 3a), high $^{206}Pb/^{204}Pb$ (18.5–18.8) and

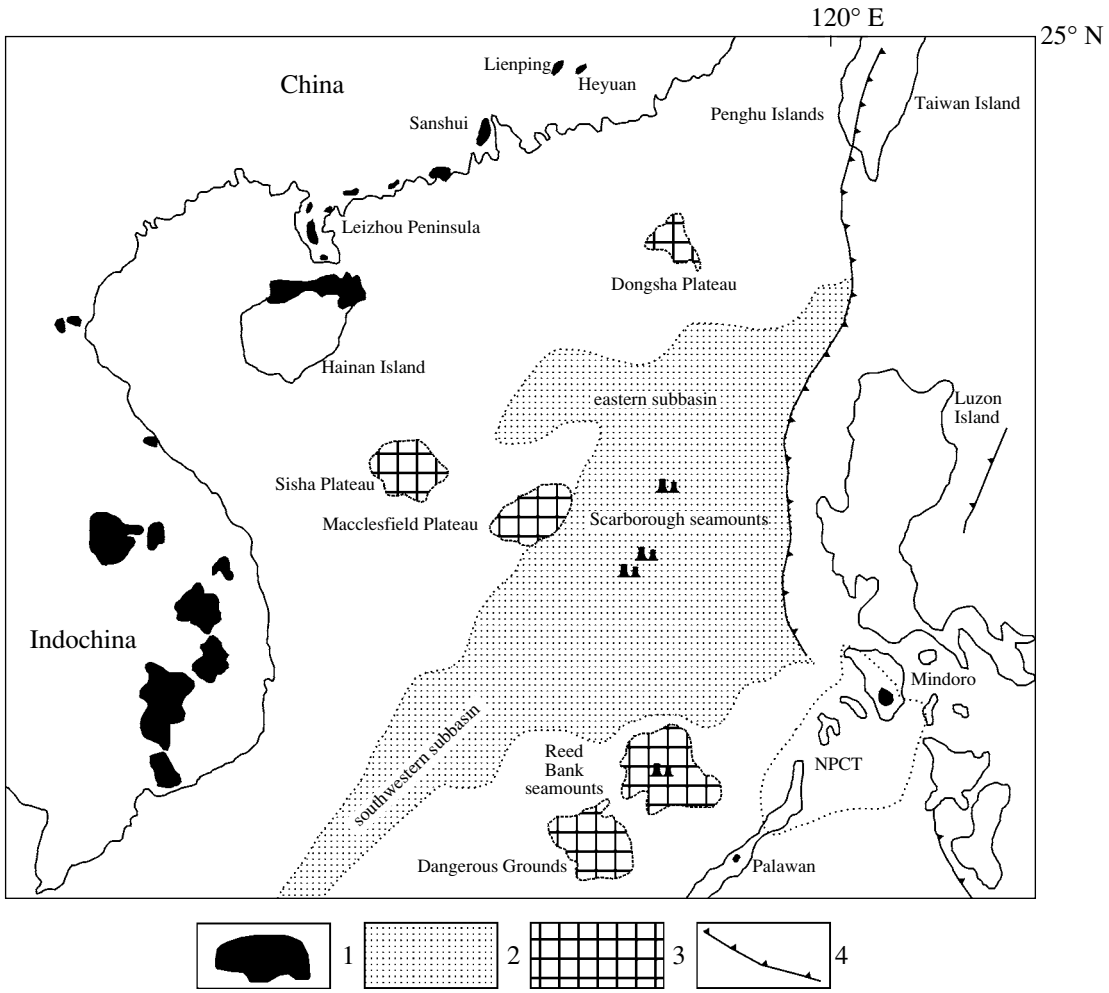

Fig. 2. Sketch map showing the distribution of Cenozoic volcanic areas in the southern China region (modified after Tu *et al.*, 1992). (1) Area of occurrence of Cenozoic basalts, (2) basin of the South China Sea, (3) submarine plateau, (4) active subduction zone, and NPCT is the North Palawan continental terrain (Taylor and Hayes, 1983).

$^{87}Sr/^{86}Sr$ (0.705–0.707) (Fig. 5a), and low $^{143}Nd/^{144}Nd$ (0.5123–0.5126) (Zhu *et al.*, 1992).

Miocene volcanics are widespread in southeastern China. They build up numerous areas in the continental part and in the islands of the Taiwan Strait, where they are represented by intercalated intraplate tholeiites and alkali basalts (Zhejiang area, Penghu Islands, etc.). There are a few areas of alkaline basaltoids (Tashan and Fangshan) and zones (Fujian province) where areas with tholeiitic volcanism in the outer parts are changed by areas with alkali olivine basalts in the middle parts and basanites and nephelinites in the interior parts (Chung *et al.*, 1994; Peng *et al.*, 1986; Zou *et al.*, 2000).

The earliest occurrences of Miocene volcanism (19.0–9.5 Ma) are known in the Zhejiang area, which is made up of intercalated flows of alkali basalts and tholeiites. These rocks have moderately depleted Sr and Nd isotopic compositions (0.70411 and 0.512932, respectively) (Fig. 5a) and moderately enriched Pb compositions: $^{206}Pb/^{204}Pb$ = 18.425–18.562, $^{207}Pb/^{204}Pb$ = 15.555–15.562, $^{208}Pb/^{204}Pb$ = 38.507–38.911 (Fig. 6), and $\Delta 8/4Pb$ = 60–85 (Peng *et al.*, 1986).[1]

The middle Miocene Tashan (16.3 Ma) and Fangshan (9.1–9.4 Ma) areas are confined to a system of nearly east–west trending strike-slip faults and grabens separating the North Chinese and Yangtze blocks. They are formed by flows of alkali basalts and basanites (Zou *et al.*, 2000), which show a strong incompatible element enrichment (Figs. 3, 4), the maximum depletion in Sr and Nd isotope compositions among the Miocene rocks of the region ($^{87}Sr/^{86}Sr$ = 0.703252–0.703396 and $^{143}Nd/^{144}Nd$ = 0.512935–0.512976) (Fig. 5a), and relatively low Pb isotope ratios: $^{206}Pb/^{204}Pb$ = 18.020–18.208,

[1] $\Delta 8/4Pb = (^{208}Pb/^{204}Pb)_i - (^{208}Pb/^{204}Pb)_{NHRL} \times 100$, where $(^{208}Pb/^{204}Pb)_{NHRL} = 1.209 \times (^{206}Pb/^{204}Pb) + 15.627$ (Hart, 1988).

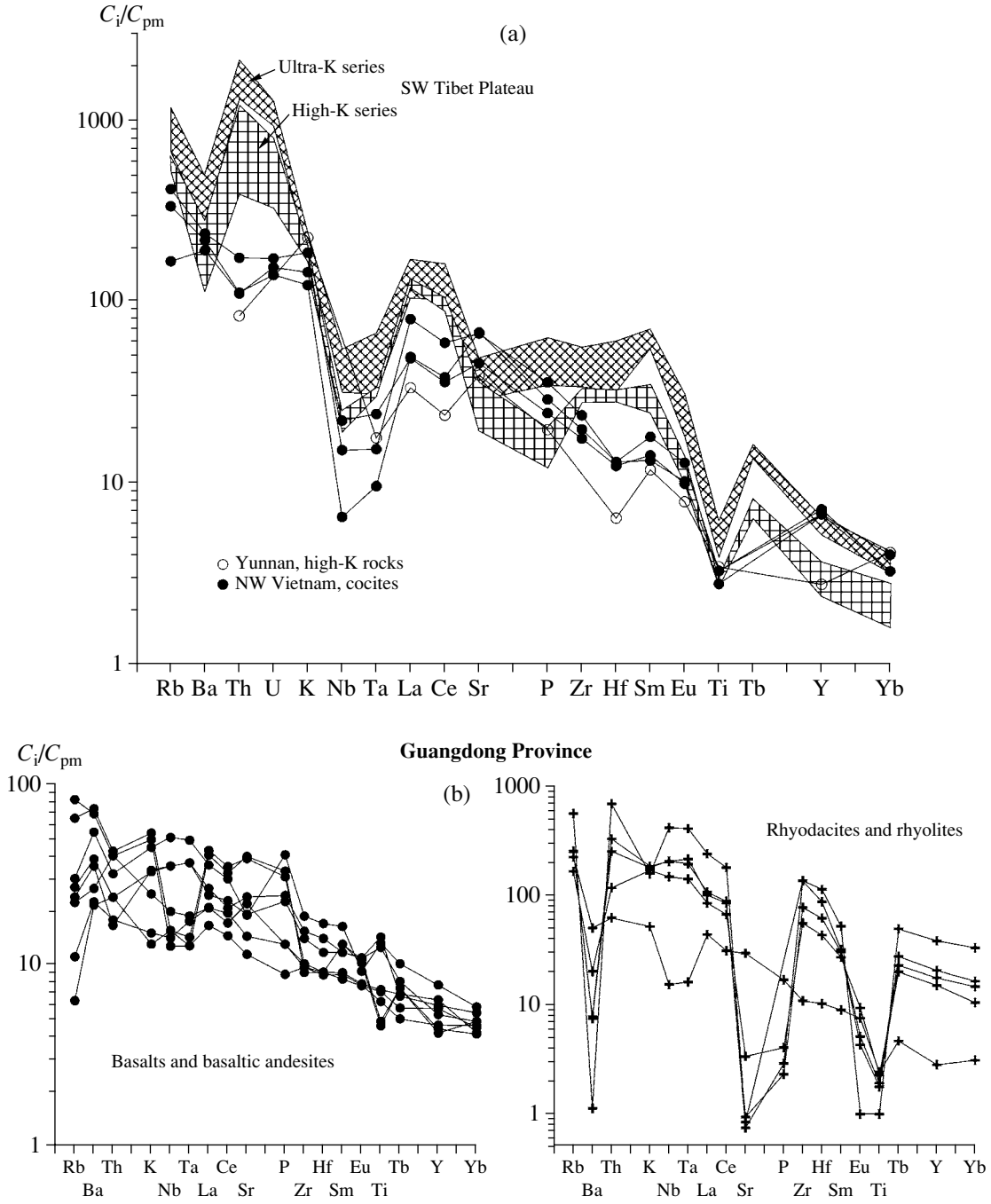

Fig. 3. Distribution of incompatible elements in the Cenozoic volcanics of the southeastern Asian margin, including southeastern China (Basu *et al.*, 1991; Fan and Hooper, 1991; Chung *et al.*, 1997; Flower *et al.*, 1992; Peng *et al.*, 1986; Zou *et al.*, 2000), South China Sea (Flower *et al.*, 1992; Tu *et al.*, 1992), Taiwan region and Okinawa Trough (Chung *et al.*, 1994, 1995; Shinjo *et al.*, 1999; Shinjo and Kato, 2000), Vietnam (our data and Hoa *et al.*, 1995; Hoang *et al.*, 1996; Hoang and Flower, 1998), and Thailand (Mukasa *et al.*, 1996; Zhou and Mukasa, 1997). The concentrations of incompatible elements in the rocks are normalized to primitive mantle (pm) (Sun and McDonough, 1989).

$^{207}Pb/^{204}Pb$ = 15.484–15.532, $^{208}Pb/^{204}Pb$ = 37.853–38.143 (Fig. 6), and $\Delta 8/4Pb$ = 43–55.

Three zones of middle–late Miocene volcanic areas were distinguished in the Fujian province (Chung *et al.*, 1994; Zou *et al.*, 2000) (from east to west): outer (Niutoushan), middle (Minqing), and inner (Miocene lava flows of the Mingxi region) confined to a northeast-trending fault system (Fig. 1). The dominant types of volcanics change from the outer to the inner zone from olivine tholeiite, through alkali olivine basalt, to basanite and nephelinite. All the rocks are enriched in

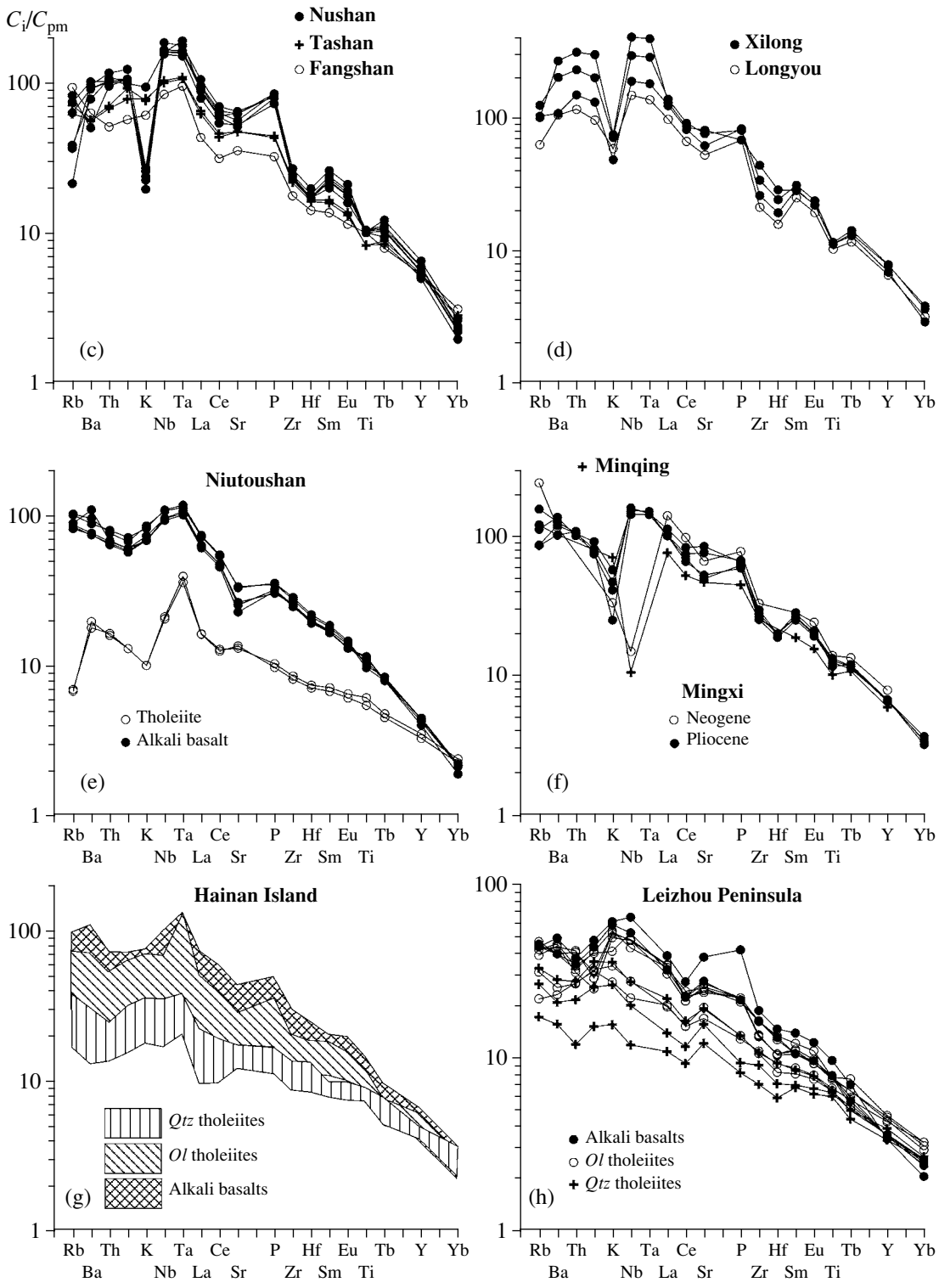

Fig. 3. (Contd.)

incompatible elements, and their geochemical characteristics correspond to intraplate-type tholeiites and alkali basalts (Sun and Lai, 1980; Chung *et al.*, 1994). The Sr and Nd isotopic ratios of all the volcanics are moderately depleted, and the basanites of the inner zone show higher $^{143}Nd/^{144}Nd$ (0.51290–0.51297) and lower $^{87}Sr/^{86}Sr$ (0.7036–0.7039) values compared with the outer zone tholeiites (0.51275–0.51285 and 0.7038–0.7043, respectively). The $^{206}Pb/^{204}Pb$ ratio increases toward the outer zone (18.2–18.6–19.0), and

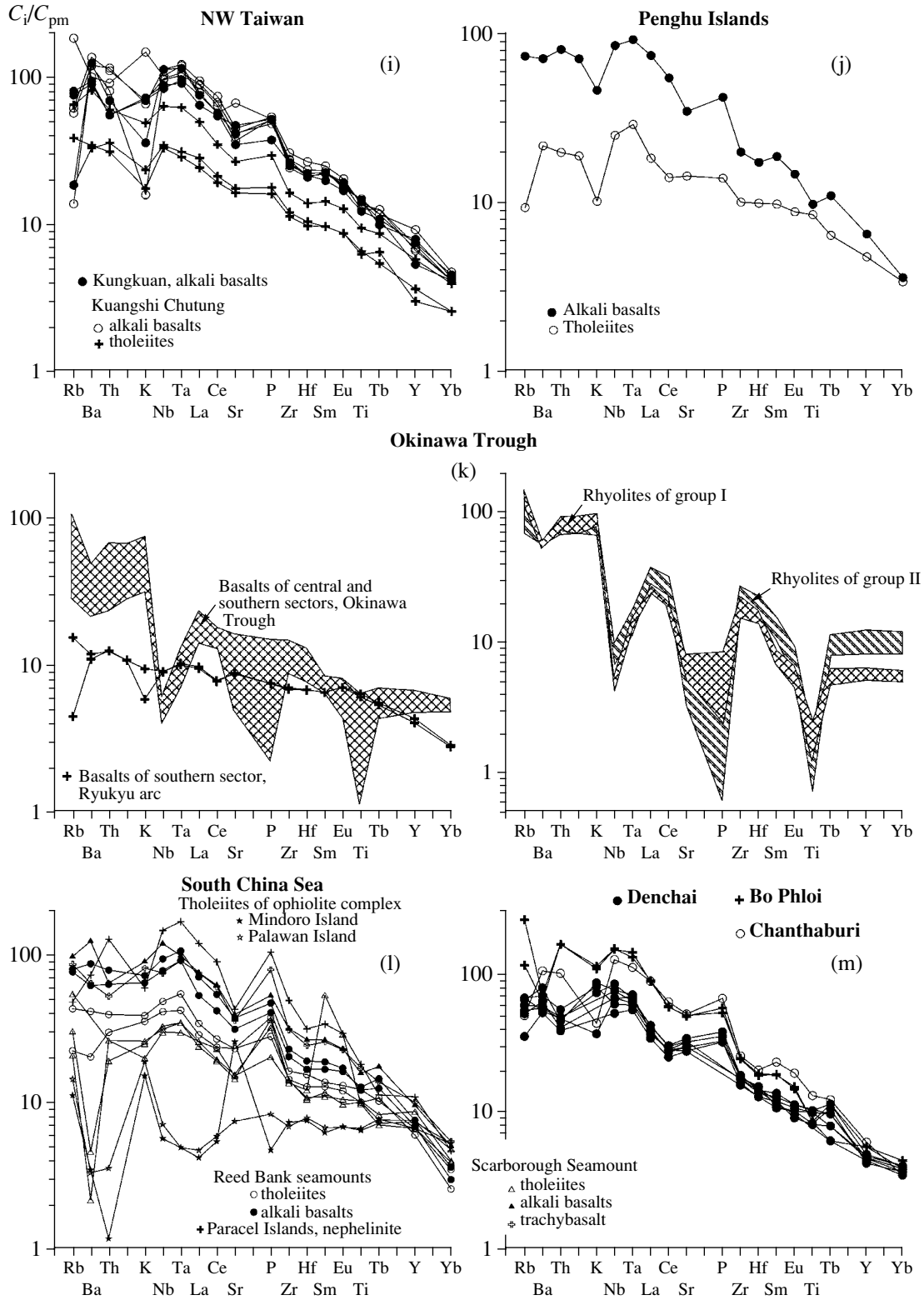

Fig. 3. (Contd.)

the Δ8/4Pb and Δ7/4Pb ratios change from 41 to 83 and from 3.7 to 10, respectively (Figs. 5a, 6).

The early Miocene alkali basalts of Kungkuan and the middle–late Miocene tholeiites and alkali basalts of the Kuangshi-Chutung area (Chung *et al.*, 1995) in northwestern Taiwan show similar distributions of incompatible elements approaching that of OIB (Fig. 3i) and strongly variable isotopic characteristics.

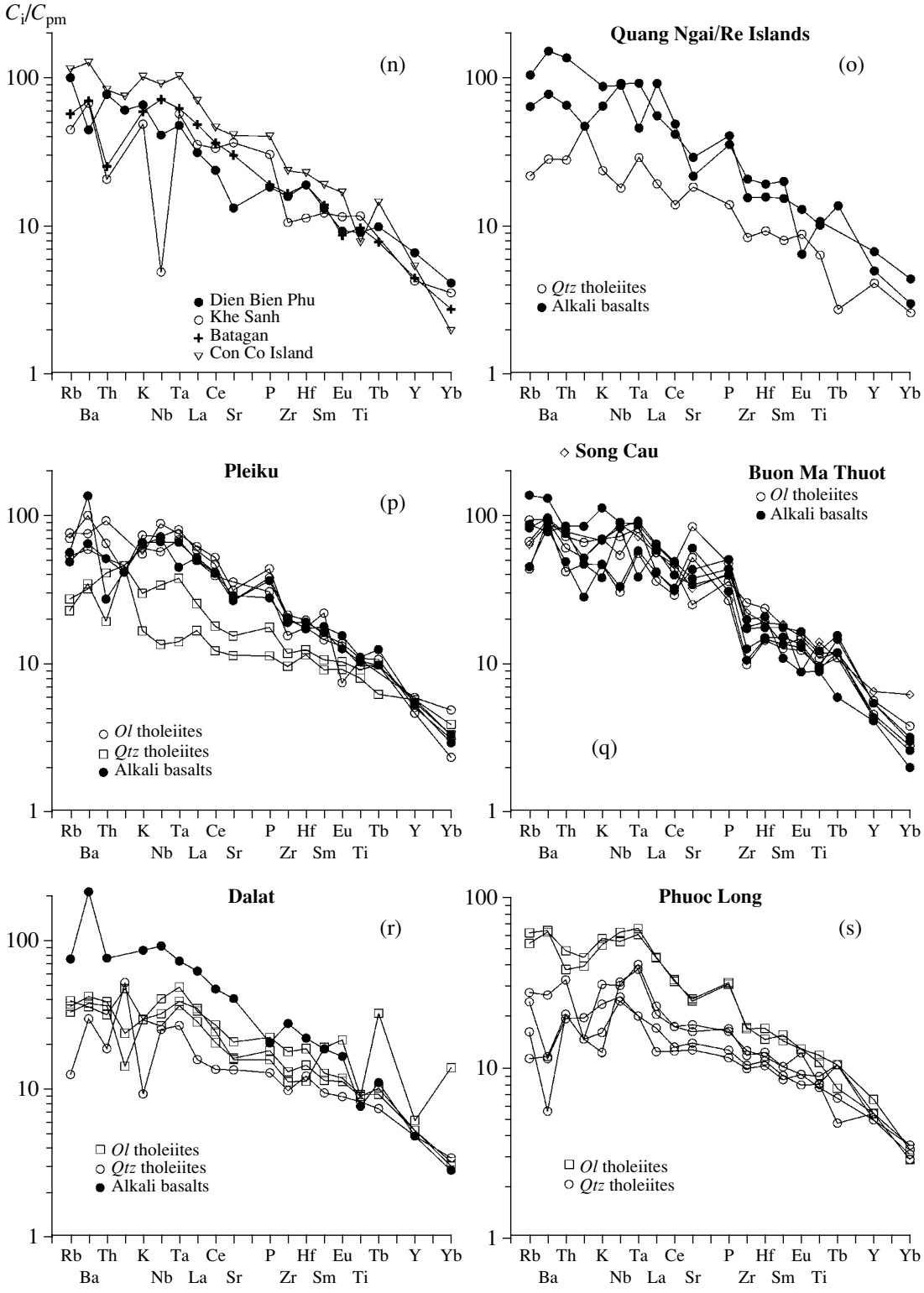

Fig. 3. (Contd.)

For instance, the Kungkuan basalts have moderately depleted Sr and Nd isotopic signatures ($^{87}Sr/^{86}Sr$ = 0.70358–0.70362 and $^{143}Nd/^{144}Nd$ = 0.51289–0.51294), and their Pb isotope ratios ($^{206}Pb/^{204}Pb$ = 18.650–18.802, $^{207}Pb/^{204}Pb$ = 15.566–15.572, $^{208}Pb/^{204}Pb$ = 38.796–38.920, and Δ8/4Pb = 55–60) suggest a contribution from the EMII component. The Kuangshi-Chutung basalts show lower $^{143}Nd/^{144}Nd$ (0.51257–0.51282),

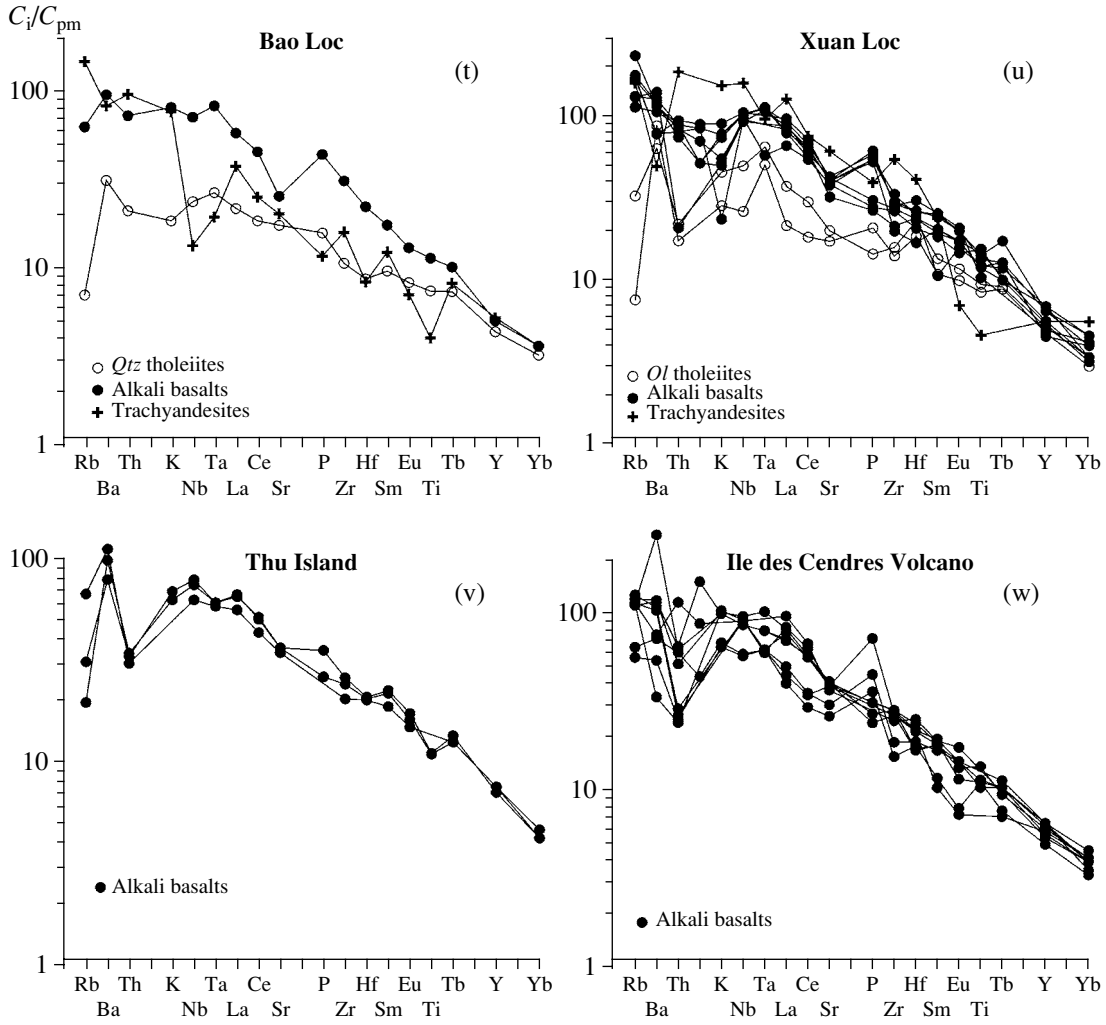

Fig. 3. (Contd.)

$^{206}Pb/^{204}Pb$ (17.654–18.342), and $^{207}Pb/^{204}Pb$ (15.557–15.629) and higher $^{87}Sr/^{86}Sr$ (0.70403–0.70559), $^{208}Pb/^{204}Pb$ (37.074–38.703), and Δ8/4Pb (75–130) ratios. The latter values are indicative of the influence of the EMI component (Figs. 5a, 6; Chung *et al.*, 1995).

The Pliocene–Quaternary volcanism of the mainland part of southeastern China was of limited extent and produced alkali basalts in the Nushan, Longyou, and Xilong areas and nephelinites and limburgites in the Mingxi area, which show a strong HFSE and LILE enrichment (Figs. 3c, 3d, 3f) and depleted isotopic compositions (Fig. 5a) (Basu *et al.*, 1991; Chung *et al.*, 1994; Zou *et al.*, 2000). The volcanic complexes of the Leizhou Peninsula and Hainan Island (Table 2) are composed of numerous flows of quartz and olivine tholeiites and scoria cones of alkaline lavas (Fan and Hooper, 1991; Kung-Suan Ho *et al.*, 2000; Tu *et al.*, 1991; etc.). All the basalts of this age are assigned to the intraplate type; the degree of their HFSE and LILE enrichment and La_n/Yb_n ratios increase from *Qtz*-normative tholeiites to *Ol*-normative tholeiites and alkali basalts. The $^{87}Sr/^{86}Sr$ ratio varies from 0.7035 to 0.7045 (Tu *et al.*, 1992), and the lower values were found in the alkali basalts (0.7035–0.7041). The $^{143}Nd/^{144}Nd$ ratio ranges between 0.51282 and 0.51293. The lead isotopic characteristics of the Hainan Island basalts (Tu *et al.*, 1992) fall within the field of DUPAL-type OIB compositions of the southern hemisphere (Hart, 1988), and the *Qtz* tholeiites have a more radiogenic composition.

CENOZOIC VOLCANISM OF THE OKINAWA TROUGH

The Okinawa Trough extends over a distance of more than 800 km and is a young intracontinental rift basin formed by a series of nearly parallel northeast-trending grabens about 10 km wide and 50–100 km long in the back zone of the Ryukyu island-arc system. Volcanic activity was confined to the Pleistocene and produced a bimodal tholeiite basalt–rhyolite association (Shinjo *et al.*, 1999). The tholeiites show differentiated distribution patterns of incompatible elements

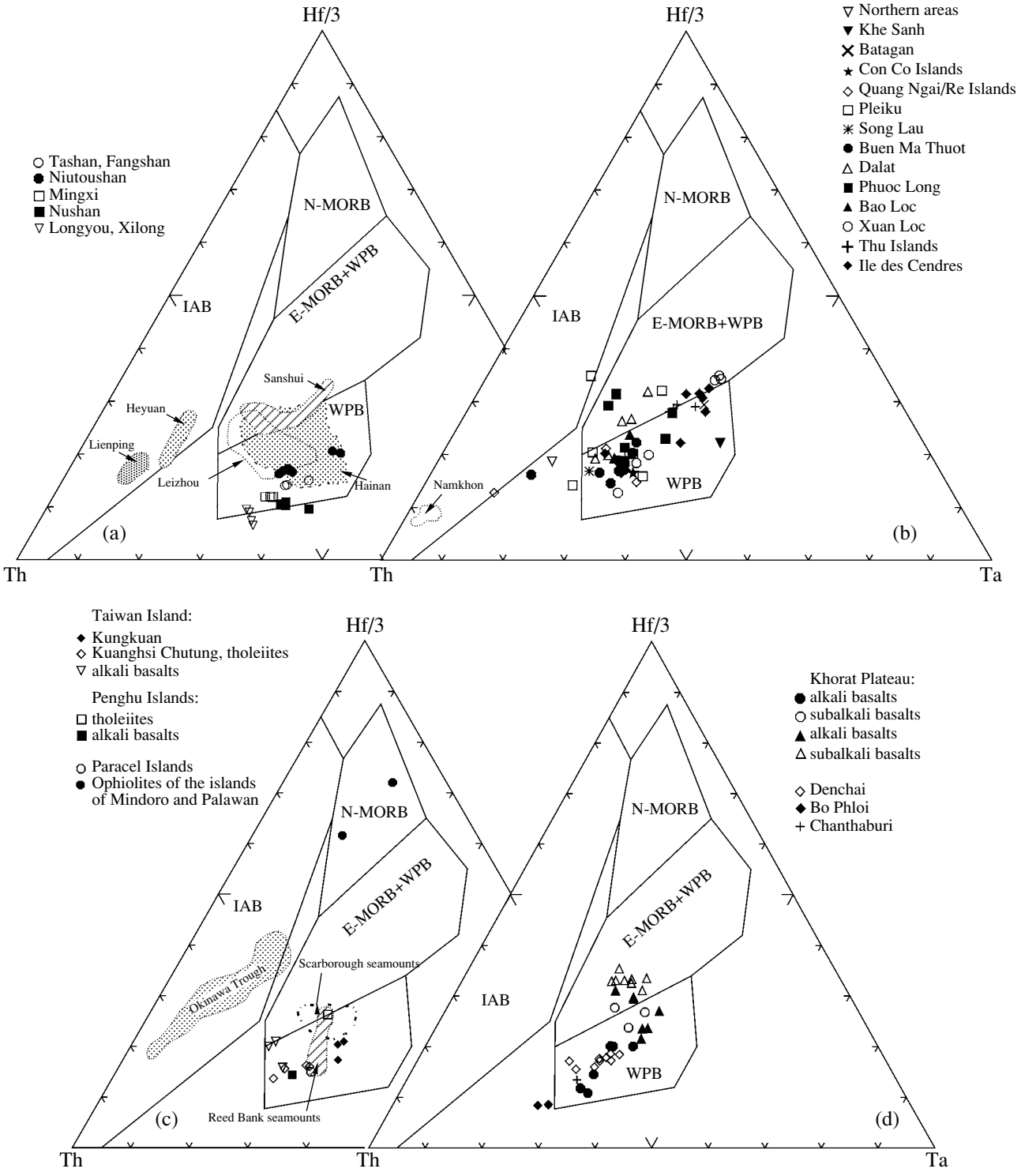

Fig. 4. Discriminant diagram Th–Hf–Ta for the Cenozoic rocks of the southeastern Asian margin: (a) southeastern China, (b) Vietnam, (c) region of the South China Sea and Okinawa Trough, and (d) western Indochina. Data sources: Southeastern China (Basu *et al.*, 1991; Fan and Hooper, 1991; Chung *et al.*, 1997; Flower *et al.*, 1992; Peng *et al.*, 1986; Zou *et al.*, 2000); South China Sea (Flower *et al.*, 1992; Tu *et al.*, 1992); Taiwan region and Okinawa Trough (Chung *et al.*, 1994, 1995; Shinjo *et al.*, 1999; Shinjo and Kato, 2000); Vietnam (our analyses and data by Hoa *et al.*, 1995; Hoang *et al.*, 1996; Hoang and Flower, 1998); and Thailand (Mukasa *et al.*, 1996; Zhou and Mukasa, 1997). Also shown are fields of basalts from various geodynamic settings (Wood, 1980): depleted tholeiites of mid-ocean ridges (N-MORB), enriched tholeiites of mid-ocean ridges and tholeiites of intraplate structures (E-MORB), alkali basalts of intraplate structures (WPB), and island arcs and active continental margins (IAB).

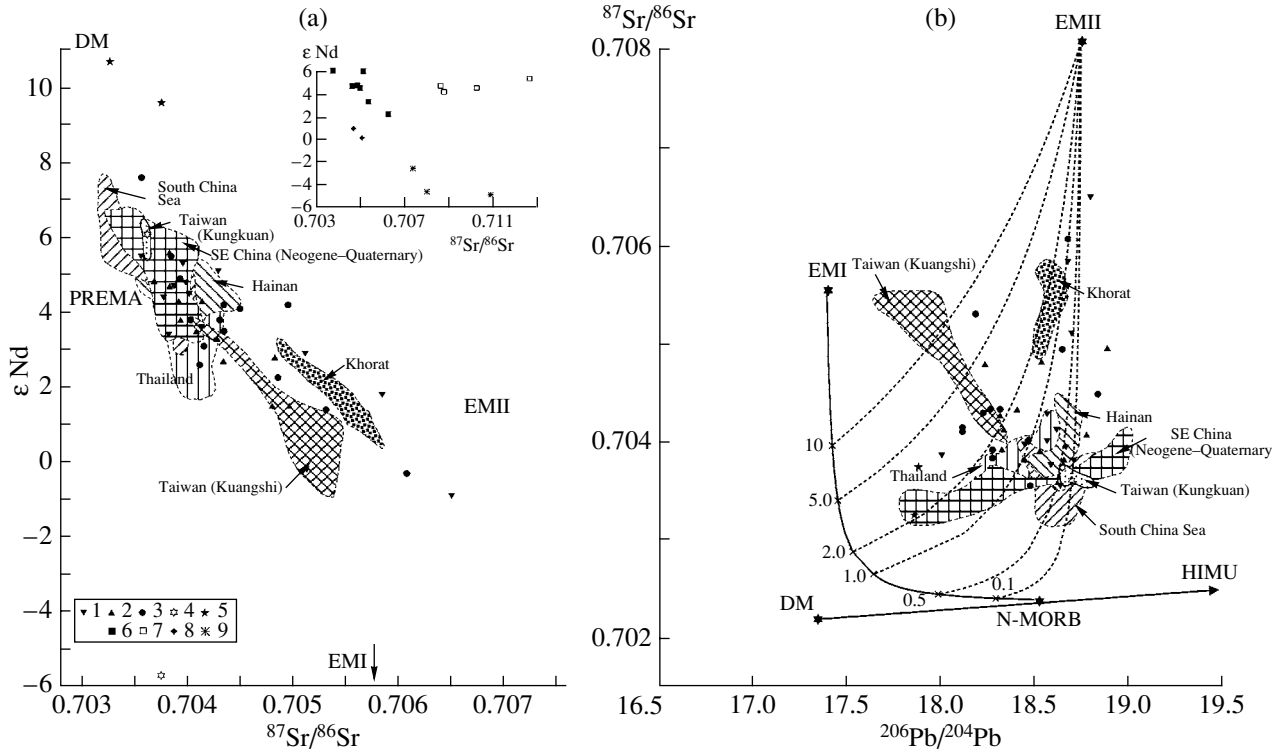

Fig. 5. Diagrams (a) $^{87}Sr/^{86}Sr$ versus εNd and (b) $^{206}Pb/^{204}Pb$ versus $^{87}Sr/^{86}Sr$ for the Cenozoic volcanics of the southeastern Asian margin. (1)–(3) Vietnam: (1) quartz tholeiite, (2) olivine tholeiite, and (3) alkali basalt; (4) Penghu Islands; (5) ophiolite complexes of the islands of Mindoro and Palawan; (6)–(9) Early Paleogene complexes of southeastern China: (6) Sanshui basalt, (7) Sanshui trachyte, (8) Heyuan, and (9) Lienping. In addition to our own data, published analyses were used (Basu *et al.*, 1991; Fan and Hooper, 1991; Chung *et al.*, 1994, 1997; Flower *et al.*, 1992; Mukasa *et al.*, 1996; Zhou and Mukasa, 1997; Peng *et al.*, 1986; Zou *et al.*, 2000). The compositions of sources are after Zindler and Hart (1986).

with LILE enrichment relative to HFSE and a pronounced Ta–Nb minimum (Fig. 3k; Table 2). The $^{87}Sr/^{86}Sr$ and $^{143}Nd/^{144}Nd$ ratios of the basalts are moderately depleted (0.703685–0.70462 and 0.512714–0.512908, respectively). The rhyolites are medium-K and form two groups with different trace and rare earth element distribution patterns: the first group shows high La_n/Sm_n (2.8–3.5) and La_n/Yb_n (3.8–4.5) and isotopic characteristics similar to those of the tholeiites, and the second group has lower La_n/Sm_n (2.2–2.7) and La_n/Yb_n (2.6–3.3) and higher $^{87}Sr/^{86}Sr$ (0.704301–0.704799) values.

CENOZOIC VOLCANISM OF THE SOUTH CHINA SEA

Early Oligocene basalts (~34 Ma; Encarnacion *et al.*, 2001) from the ophiolite complex of the islands of Mindoro and Palawan (Fig. 2) can be regarded as relics from an early event of South China Sea spreading (Tu *et al.*, 1992). The basalts are olivine (Mindoro) and quartz (Palawan) tholeiites, which fall within the N-MORB field in the Hf–Ta–Th diagram (Fig. 4c). They show depleted HFSE and REE distribution patterns (La_n/Sm_n = 0.63–0.66 and La_n/Yb_n = 0.7–0.8; Fig. 3l), high $^{143}Nd/^{144}Nd$ (0.5131), and low $^{87}Sr/^{86}Sr$ (0.703264–0.703754), $^{206}Pb/^{204}Pb$ (17.86–17.88) (Fig. 5a), and $^{208}Pb/^{204}Pb$ (37.61–37.65) (Fig. 6b) ratios similar to those from the East Taiwan ophiolite (Jahn, 1986).

The postspreading volcanism of the South China Sea is represented by the basaltoids of the Scarborough seamounts, Reed Bank, and Paracel Islands (Fig. 2) (Tu *et al.*, 1992).

The basalts of the Scarborough seamounts are olivine tholeiites (13.9 Ma), trachybasalts and olivine tholeiites (9.9 Ma), and alkali olivine basalts (3.5 Ma) (Tu *et al.*, 1992; Wang *et al.*, 1986). The volcanism of the Reed Bank occurred in the Pliocene–Quaternary (0.5–2.7 Ma) (Kudrass *et al.*, 1986) and produced tholeiites and alkali basalts. The tholeiites show a moderate incompatible element enrichment and fractionated REE distribution patterns (La_n/Sm_n = 2.0–2.1 and La_n/Yb_n = 4.9–6.1), whereas the trachybasalts and alkali olivine basalts are strongly enriched in incompatible elements and REE (La_n/Sm_n = 2.5–2.7 and La_n/Yb_n = 12.5–13.7). The $^{87}Sr/^{86}Sr$ ratios of the Scarborough tholeiites are relatively low (0.703176–0.703192), and $^{143}Nd/^{144}Nd$ is moderately high (0.512916–0.512929); the alkali basalts show more enriched isotopic characteristics (0.703898–0.703909 and 0.512791–0.512813,

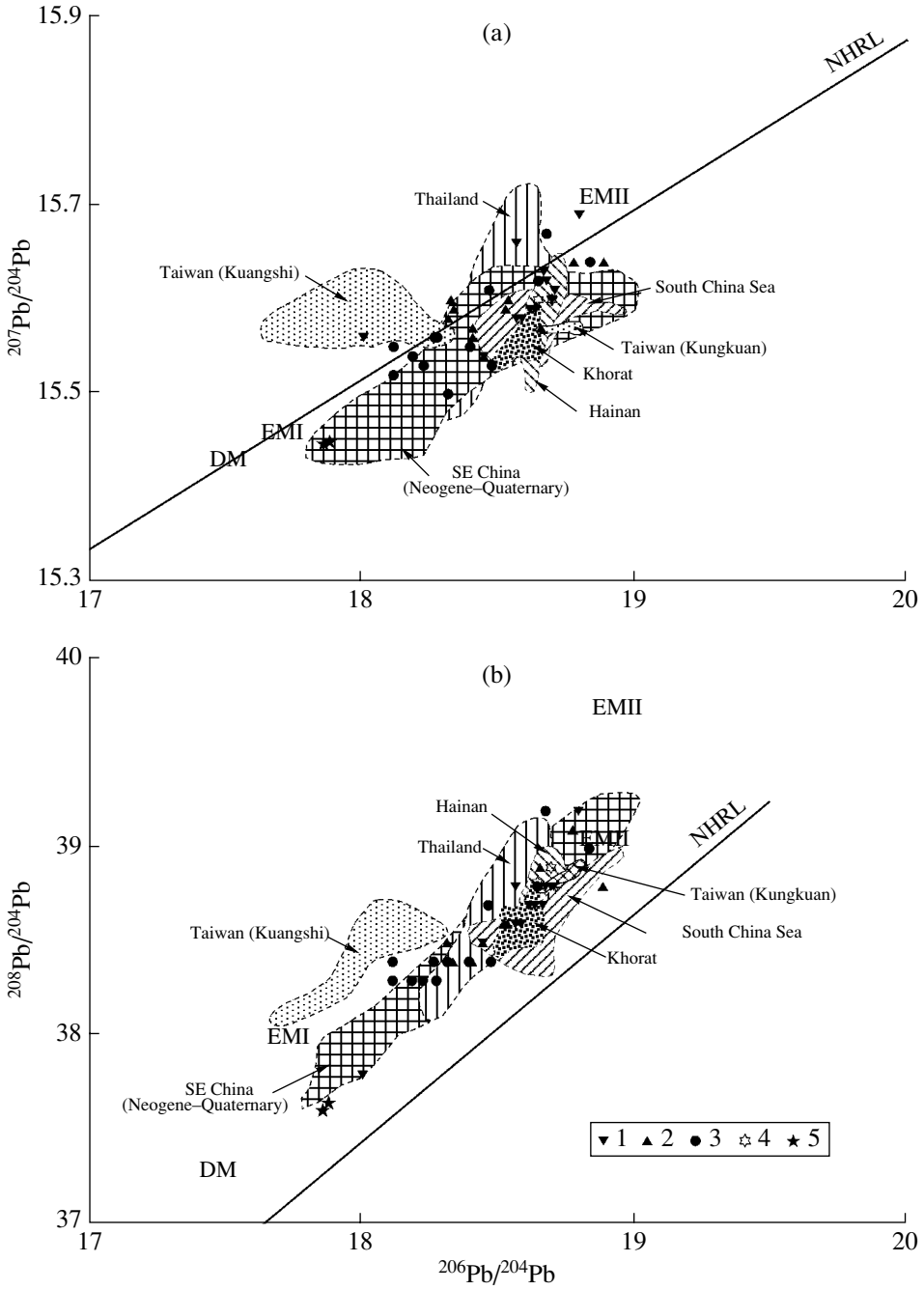

Fig. 6. Variations of $^{207}Pb/^{204}Pb$, $^{208}Pb/^{204}Pb$, and $^{206}Pb/^{204}Pb$ ratios in the Cenozoic volcanics of the southeastern Asian margin. (1–3) Vietnam: (1) quartz tholeiite, (2) olivine tholeiite, and (3) alkali basalt; (4) Penghu Islands; and (5) ophiolite complexes of the islands of Mindoro and Palawan. The data are after (Basu *et al.*, 1991; Fan and Hooper, 1991; Chung *et al.*, 1994, 1997; Flower *et al.*, 1992; Mukasa *et al.*, 1996; Zhou and Mukasa, 1997; Peng *et al.*, 1986; Zou *et al.*, 2000). The compositions of sources are after Zindler and Hart (1986).

respectively). The Sr and Nd isotopic ratios of tholeiites and alkali basalts from the Reed Bank are similar to each other (0.70343–0.7040 and 0.51288–0.51292, respectively) (Fig. 5a). The $^{206}Pb/^{204}Pb$ values of the Scarborough basalts increase regularly from the olivine tholeiite (18.6–18.7), through trachybasalt (18.95), to alkali olivine basalt (19.03), whereas the Reed Bank basalts show a decrease in $^{206}Pb/^{204}Pb$ from tholeiite (18.54–18.60) to alkali basalt (18.41–18.48) (Figs. 6a, 6b).

The Late Cenozoic volcanism of the Paracel Islands is represented by nephelinites with a strong incompatible element enrichment and highly fractionated REE distribution patterns (La_n/Sm_n = 3.3 and La_n/Yb_n = 23.4). Their $^{87}Sr/^{86}Sr$ (0.703218), $^{143}Nd/^{144}Nd$ (0.513035), and

Table 1. Representative compositions of Cenozoic volcanics from southeastern China

Component	Sanshui*		Fangshan–Tashan		Niutoushan		Mingxi		Nushan	Xilong	Longyou	Leizhou			Hainan		
	1	2	3	4	5	6	7	8	9	10	11	12	13	14	15	16	17
	KS-10**	K-50	Fang-1	Ta-1	NT-1	NT-26	M-23	M-36	Ns-30	Xi-65	Long-1	HK29	HK40	HK33	34	75	12
SiO_2	48.85	65.14	47.60	47.70	50.52	48.90	42.30	42.90	44.80	43.10	44.20	53.61	52.22	48.58	51.72	51.92	46.76
TiO_2	2.84	0.42	2.21	1.82	1.36	2.34	2.89	2.78	2.24	2.53	2.31	1.37	1.68	2.10	1.75	1.95	2.47
Al_2O_3	15.29	15.69	14.30	14.89	15.81	15.03	10.01	9.83	14.48	12.34	12.10	15.32	15.35	14.97	14.52	14.65	14.38
Fe_2O_3	13.98	5.02	11.56	11.40	11.73	11.52	13.28	12.84	13.76	12.49	12.67	–	–	–	2.96	4.99	7.54
FeO	–	–	–	–	–	–	–	–	–	–	–	9.08	9.81	10.74	8.27	6.10	4.59
MnO	0.20	0.12	0.18	0.19	0.18	0.16	0.21	0.18	0.21	0.19	0.22	0.13	0.15	0.16	0.15	0.14	0.17
MgO	4.57	0.25	10.14	9.22	7.57	8.69	16.84	16.09	9.37	10.71	11.54	7.70	6.75	7.23	7.04	6.89	7.55
CaO	9.17	1.04	7.64	8.33	9.64	7.55	10.31	11.02	8.56	8.60	10.23	8.35	8.04	7.83	8.51	8.24	9.05
Na_2O	3.36	5.67	3.72	3.62	2.51	3.37	0.95	1.78	4.21	5.64	3.55	2.85	3.64	3.80	2.86	3.06	2.40
K_2O	1.34	5.61	1.87	2.34	0.31	2.12	1.46	0.78	0.83	2.33	1.83	0.80	1.64	1.86	0.82	1.01	1.77
P_2O_5	0.69	0.05	0.56	0.77	0.18	0.53	1.18	1.04	1.41	1.20	1.20	0.16	0.36	0.72	0.23	0.33	0.73
LOI	–	–	–	–	–	–	–	–	–	–	–	0.13	0.31	1.04	–	–	–
Total	100.29	99.01	99.78	100.28	99.81	100.21	99.43	99.24	99.87	99.13	99.85	99.50	99.95	99.03	98.83	99.28	97.41
Sc	–	–	–	–	–	–	–	–	–	–	–	20.4	16.7	13.6	25	21	21
Cr	–	–	–	–	–	–	–	–	–	–	–	237	184	132	218	243	207
Ni	–	–	–	–	–	–	–	–	–	–	–	193	168	139	158	173	195
Co	–	–	–	–	–	–	–	–	–	–	–	54	51	43	59	55	55
Rb	19	161	60.4	40.2	4.52	56.4	103	73.7	23.7	66.1	41.3	17	28	28	16	20	39
Sr	395	16	761	1015	283	572	1667	1149	1389	1762	1148	331	535	811	306	401	762
Ba	378	55	449	406	128	548	916	991	688	1940	760	147	280	346	127	160	765
Hf	5.2	27.1	4.45	5.24	2.35	6.33	6.35	6.01	6.2	9.19	5.06	2.20	4.16	4.56	2.67	3.89	6.01
Zr	207	1519	202	257	98	294	322	293	306	509	246	102	183	211	121	152	250
Y	35	94	24.5	24.6	16.4	20.4	30.7	31.6	30.1	36.5	30.9	17.8	21.2	15.5	21.2	24.2	30.6
Ta	2	8.9	3.98	4.57	1.66	4.52	6.28	6.08	7.44	16.7	5.8	–	–	–	0.85	1.31	4.89
Nb	36	146	61.1	75.3	15.5	69.3	115	106	135	299	109	14.4	31	46.6	16.9	24.4	69.6
Th	2.7	28.1	4.42	6.09	1.43	5.87	9.3	8.89	10.1	27.4	10.2	1.85	2.77	3.22	1.73	2.44	6.18
U	–	–	1.22	1.98	0.28	1.3	1.76	1.7	2.64	6.49	2.09	0.54	0.87	1.01	0.40	0.60	0.95
La	24.4	69.2	30.3	45.5	11.5	44.6	72.3	71.7	73.7	92.2	69.2	9.6	23.0	26.9	11.8	17.5	50.1
Ce	52.8	152	56.7	83	23.4	86.4	137	121	126	156	122	20.7	43.3	49.1	25.30	34.80	101.50
Pr	–	–	6.73	9.33	3	10.2	16.5	15.8	15	18	14.5	–	–	–	–	–	–
Nd	27.2	66.2	27.2	36.1	12.8	39.3	64.2	61.5	58.5	67.7	57.1	11.2	25.6	29.8	14.1	20.4	39.2
Sm	7.2	14.2	6.17	7.5	3.25	7.84	12	11.5	11.8	13	11.5	3.1	5.4	6.2	3.83	5.36	7.92
Eu	1.54	0.87	1.96	2.34	1.12	2.38	3.4	3.33	3.61	3.84	3.37	1.12	1.85	2.07	1.39	1.93	2.78
Gd	–	–	5.77	6.63	3.31	6.61	9.7	9.45	10	10.8	9.73	–	–	–	–	–	–
Tb	1.09	3.00	0.87	0.97	0.53	0.91	1.29	1.25	1.34	1.50	1.30	0.54	0.82	0.76	0.85	0.79	0.77
Dy	–	–	4.63	4.84	3.04	4.37	6.17	6.05	6.36	7.48	6.34	–	–	–	–	–	–
Ho	–	–	0.85	0.85	0.58	0.73	1.07	1.05	1.04	1.28	1.08	–	–	–	–	–	–
Er	–	–	2.08	2.01	1.50	1.64	2.49	2.50	2.25	2.95	2.48	–	–	–	–	–	–
Yb	2.87	8.18	1.56	1.41	1.21	1.10	1.76	1.72	1.31	1.96	1.63	1.33	1.61	1.02	1.50	1.61	1.82
Lu	0.42	1.16	0.21	0.19	0.17	0.15	0.24	0.23	0.16	0.25	0.21	0.20	0.22	0.11	0.22	0.21	0.23

Note: Analyses (1), (3), (4), (6)–(11), (14), and (17) are alkali basalts; (2) trachyte; (3), (13), and (16) olivine tholeiites; (12) and (15) quartz tholeiites. Analyses (1) and (2) are after Chung *et al.* (1997); (3)–(11) after Zou *et al.* (2000); (12)–(14) after Kung Suan Ho *et al.* (2000); and (15)–(17) after Flower *et al.* (1992). Here and in Tables 2–4, oxides are in wt % and elements are in ppm; dashes denote not determined.

* Here and in Tables 2–4, area.

** Here and in Tables 2–4, sample number.

Table 2. Representative analyses of Cenozoic volcanics from the East China Sea

Component	NE Taiwan*			Penghu Islands		Okinawa Trough			
	1	2	3	4	5	6	7	8	9
	TB-07**	N-209	S-03	PH-89	PH-96	CB6-22	A7B	12-2YK	DR8-2
SiO_2	46.97	46.46	52.00	51.64	44.87	49.20	51.10	72.11	71.01
TiO_2	3.16	2.82	1.46	1.86	2.14	0.96	1.38	0.35	0.36
Al_2O_3	16.15	13.58	14.08	14.21	12.79	16.82	16.80	14.44	14.32
Fe_2O_3	12.21	10.47	9.79	11.60	12.62	9.69	10.11	2.68	3.74
MnO	0.17	0.16	0.14	0.15	0.19	0.16	0.19	0.07	0.10
MgO	4.88	9.19	6.87	7.33	11.48	7.68	5.34	0.51	0.44
CaO	7.31	8.32	8.53	9.49	9.57	11.33	9.63	2.20	2.13
Na_2O	3.94	3.48	3.01	2.66	2.38	2.15	3.36	4.15	4.98
K_2O	2.16	2.13	0.54	0.31	1.40	0.42	0.60	2.67	2.51
P_2O_5	0.89	0.84	0.28	0.24	0.72	0.16	0.24	0.07	0.07
LOI	1.35	1.84	2.84	–	–	0.56	1.07	–	–
Total	99.19	99.29	99.54	99.49	98.162	99.13	99.82	99.25	99.66
Cr	28	247	270	208	449	246	22	3	4
Ni	39	204	45	161	333	83	18	2	1
Co	42	49	45	–	–	41	34	3	3
Sc	15	21	16	25	24	38	34.7	4.8	9.7
Rb	49	40	25	6	47	8.8	14	82.1	48.6
Ba	639	971	245	153	500	75	114	396	385
Sr	883	897	352	306	738	249	324	125	122
U	–	–	–	0.4	1.5	0.21	0.29	1.72	1.45
Th	4.8	9.6	2.7	1.7	6.9	0.67	1.06	7.08	5.82
Ta	4	4.5	1.2	1.2	3.8	0.23	0.26	0.6	0.63
Nb	61	71	24	18	61	3.5	4	6.6	9.1
Hf	7	6.7	3.1	3.1	5.4	1.48	2.06	4.29	6.64
Zr	286	312	130	114	225	58	85	177	295
Y	35	31	17	22	30	21.1	28.2	23.5	47.7
La	52.8	62.8	17	12.7	51.3	5.51	9.54	16.2	22.14
Ce	103	122	34.9	25.2	97.8	13.22	22.43	32.46	49.21
Pr	–	–	–	–	–	1.92	3.15	3.75	6.05
Nd	53	55.1	17.7	16.2	45	9.2	14.39	14.22	24.69
Sm	10.2	10	4.4	4.4	8.4	2.66	3.81	3.08	5.87
Eu	3.3	3.2	1.5	1.5	2.5	1.03	1.36	0.81	1.35
Gd	–	–	–	–	–	3.1	4.24	3.09	6.1
Tb	1.2	1.4	0.6	0.7	1.2	0.54	0.72	0.53	1.06
Dy	–	–	–	–	–	3.44	4.49	3.33	6.81
Ho	–	–	–	–	–	0.73	0.96	0.73	1.49
Er	–	–	–	–	–	2.11	2.78	2.26	4.58
Tm	–	–	–	–	–	0.32	0.42	0.38	0.74
Yb	2.3	2.1	1.3	1.7	1.8	1.97	2.64	2.51	4.83
Lu	0.35	0.31	0.21	0.27	0.28	0.31	0.41	0.41	0.77

Note: Analyses (1), (2), and (5) are alkali basalts; (3), (4), (6), and (7) tholeiites; (8) and (9) rhyolites. Analyses (1)–(3) are after Chung *et al.* (1995); (4) and (5) after Chung *et al.* (1994); (6) and (7) after Shinjo *et al.* (1999); (8) and (9) after Shinjo and Kato (2000).

$^{208}Pb/^{204}Pb$ (38.4) ratios are similar to those of basalts from the Southeast Indian Ridge (Tu *et al.*, 1992).

CENOZOIC VOLCANISM OF INDOCHINA AND THAILAND

The Cenozoic volcanic complexes of Indochina are located in four sectors (Koloskov *et al.*, 1989; Novikov *et al.*, 1989; Hoang *et al.*, 1996; Hoang and Flower, 1998; Lee *et al.*, 1998). The northern sector includes the Oligocene Pusamkap area (outside the map), the Quaternary occurrences of Dien Bien Phu, Phu Quy, Khe Sanh, and Con Co Island (Pleistocene), and a number of small areas in Laos (Fig. 1). The central sector comprises the areas of Buon Ma Thuot (with volcanic occurrences of 3.3–4.6 and 0.3–1.9 Ma), Batagan, Song Cau (Pliocene–Quaternary), Pleiku (2.6–4.8 and 0.6–2.5 Ma), and Quang Ngai/Re Island (12 and 0.4–1.2 Ma). The southwestern sector includes the largest volcanic area of Indochina, Phuoc Long (15.0–15.1 and about 5 Ma). A number of small areas were described in the central and western parts of Cambodia and Thailand (Barr and Macdonald, 1981). The southeastern sector includes the Dalat (10.5–22.5 and <1.8–2.6 Ma) and Xuan Loc volcanic centers (2.2–2.42 and 0.4–1.1 Ma) and the Katuik (Ile des Cendres Volcano of middle Pleistocene–Recent age) and Thu (Pleistocene) volcanic islands.

The earliest occurrences of postsubduction Cenozoic volcanism in Vietnam are represented by the basic ultrapotassic rocks (cocites and absarokites) of the Pusamkap province (Dovzhikov *et al.*, 1965) related to the Shongda rift structure. With respect to chemical composition (Hoa *et al.*, 1995; Polyakov *et al.*, 1997), these igneous complexes are classed as high-magnesium, low-aluminum, highly alkaline, and low-titanium melanocratic mafic rocks (Table 3). They show an enrichment in Cs, Rb, Ba, Th, La, Sr, and Zr; a depletion in Ta, Nb, and Y; and high La_n/Yb_n ratios, which makes them similar to Mediterranean-type low-titanium lamproites from activated structures in fold belts and craton margins (Bogatikov *et al.*, 1991).

The Miocene–Holocene volcanic centers of Vietnam are related to extensional structures bounded by normal faults (Rangin *et al.*, 1995) and strike-slip faults. Some volcanic areas of Vietnam were formed by two stages of volcanic activity. The lower complex in these volcanic areas is usually composed of flows of quartz and olivine tholeiites with minor alkali basalts produced by fissure eruptions confined to major faults. The rocks of the upper complex are alkali olivine basalts, basanites, and occasional nephelinites and trachybasalts, which form central-type edifices along strike-slip faults (Table 3). Such patterns were detected in the majority of composite areas, except for Buon Ma Thuot, where the opposite sequence was found (Hoang and Flower, 1998).

The volcanic areas of the northern sector of Vietnam include scoria cones and less common individual lava flows. Basalts from the continental portions of the areas (Dien Bien Phu, Phu Quy, and Khe Sanh) are mainly *Ol*-normative and, occasionally, *Hyp*-normative tholeiites; some cones of the Khe Sanh area are made up of alkali basalt. The tholeiites are characterized by elevated alkalinity ($Na_2O + K_2O$ = 3.7–5.0 wt %), high P_2O_5 (0.3–0.5 wt %), and moderately high TiO_2 contents (1.5–2.0 wt %). The rocks are enriched in HFSE and LILE, and their spider diagrams display a Ta–Nb maximum (Fig. 3n). They show high Zr/Y values (4.4–5.9). In the Th–Hf–Ta diagram, the Khe Sanh tholeiites plot within the field of intraplate basalts, whereas the Dien Bien Phu tholeiites fall between the fields of active continental margins and intraplate basalts (Fig. 4b). The REE distribution of the tholeiites is fractionated (La_n/Sm_n = 2.3–2.7 and La_n/Yb_n = 6.9–9.1).

The quartz tholeiites of Dien Bien Phu are distinguished by high $^{87}Sr/^{86}Sr$ (0.706511) and $^{206}Pb/^{204}Pb$ (18.800) and low $^{143}Nd/^{144}Nd$ (0.512591), whereas the *Ol* tholeiites of Khe Sanh show more depleted characteristics ($^{87}Sr/^{86}Sr$ = 0.704084, $^{143}Nd/^{144}Nd$ = 0.512819, and $^{206}Pb/^{204}Pb$ = 18.780) (Fig. 5a, 6a; Hoang *et al.*, 1996). The alkali olivine basalts and basanites of Khe Sanh show moderately high alkali contents. Their incompatible element concentrations are higher than those of the olivine tholeiites, except for Ta, which shifts the points of the basanites toward the E-MORB field in the Th–Hf–Ta diagram (Fig. 4b).

The scoria cones of Con Co Island, which is situated on the continental shelf, are made up of Pleistocene alkali olivine basalts and basanites and have moderately high concentrations of alkalis and titanium. The rocks are rich in incompatible elements, and their spider diagram patterns (Fig. 3n) are similar to those of OIB. In the Th–Hf–Ta diagram (Fig. 4b), the points of these rocks plot within the WPB field. Their REE distribution patterns are strongly fractionated, and the La_n/Sm_n and La_n/Yb_n ratios (3.5 and 33, respectively) are similar to those of intraplate alkali basalts of continental rifts (Hart *et al.*, 1989). The Con Co alkali basalt shows $^{87}Sr/^{86}Sr$ = 0.703564, $^{143}Nd/^{144}Nd$ = 0.513026, and $^{206}Pb/^{204}Pb$ = 18.48 (Figs. 5a, 6; Hoang *et al.*, 1996).

The Pleiku area in the central sector of Vietnam is made up of basaltoids related to two episodes of volcanic activity. The lower complex (2.6–4.8 Ma; Hoang *et al.*, 1998) includes flows of *Qtz*- and *Ol*-normative tholeiites with minor low-titanium alkali basalts. The tholeiites show highly variable MgO (5–8 wt % in the *Qtz* tholeiites and 8–12 wt % in the *Ol* tholeiites) and SiO_2 contents. The tholeiites are rich in incompatible elements (Fig. 3p). The *Ol* tholeiites are either slightly enriched in Ta and Nb or show no anomaly, whereas some *Qtz* tholeiites display a Ta–Nb minimum. In the Th–Hf–Ta diagram (Fig. 4b), the points of the tholeiites occur within the WPB field. The distribution of REE is fractionated: the La_n/Sm_n and La_n/Yb_n ratios vary

Table 3. Representative analyses of Cenozoic volcanics from Vietnam

Component	Northern sector						Central sector			
	Namkhon*		Cocpia	Sincao	Khe Sanh	Dien	Buen Ma Thuot		Pleiku	
	1	2	3	4	5	6	7	8	9	10
	G916**	P55	G942	T1597	9-85	DBP-1	23-85b	45-5	90-15	15-85
SiO_2	50.29	48.01	52.11	49.48	47.19	54.69	45.14	45.13	54.34	49.14
TiO_2	0.72	0.57	0.61	0.72	2.61	2.02	1.95	2.68	1.80	2.34
Al_2O_3	11.09	10.6	11.53	11.56	14.22	15.84	14.94	13.53	14.50	14.08
Fe_2O_3	7.71	6.07	8.01	8.20	–	–	7.39	–	–	2.29
FeO					10.54	9.56	5.24	11.25	9.23	9.20
MnO	0.14	0.13	0.14	0.16	0.15	0.16	0.13	0.17	0.20	0.15
MgO	12.94	10.84	12.79	12.85	8.39	5.30	6.68	8.95	6.32	8.57
CaO	7.60	11.09	6.92	7.16	9.20	6.09	7.86	9.86	8.43	8.88
Na_2O	1.79	0.58	2.07	2.38	3.01	2.97	4.12	3.33	2.84	2.90
K_2O	5.71	5.96	4.46	3.78	1.50	2.02	3.43	1.16	0.52	1.98
P_2O_5	0.62	0.60	0.42	0.50	0.53	0.32	0.87	0.75	0.20	0.49
LOI	1.18	4.42	0.82	2.94	2.21	0.87	3.54	2.31	1.40	0.40
Total	99.79	98.87	99.88	99.73	99.55	99.84	101.29	99.12	99.78	100.42
Sc	–	–	–	–	17.8	15.9	–	22.8	22.9	–
Cr	–	–	–	–	213	119	253	246	199	–
Ni	–	–	–	–	134	110	153	221	111	–
Rb	270	210	108	217	29	65	56	88	15	37
Sr	1430	13858	979	1452	787	287	923	803	249	630
Ba	1690	420	1366	1553	481	318	549	924	250	980
Hf	4.1	4.1	3.9	4.1	3.60	6.00	6.50	5.50	3.70	6.10
Zr	269	299	200	225	122	182	225	196	112	220
Y	31	0.2	31	33	20.0	31.0	19.0	25.0	27.0	26.0
Ta	0.64	0.4	1.0	0.4	2.40	2.00	3.60	3.80	0.60	1.90
Nb	11	8.5	16	4.7	3.6	30	65	60	10	52
Th	3.7	5.8	3.3	3.0	1.80	6.70	7.30	6.90	1.70	2.40
U	15.1	14.2	9.6	9.7		1.30	1.80	1.00	1.00	–
La	56	142	34	34.6	24.9	22.0	29.0	44.7	11.9	37.0
Ce	107	189	65	69	60.8	43.3	56	87.8	22.6	76
Pr	–	–	–	–	–	–	–	–	–	–
Nd	46	52	32	32	25.9	22.5	24.0	37.8	13.4	42.0
Sm	8.1	8.3	6.4	6.1	5.6	6	4.9	7.9	4.2	7.5
Eu	2.20	2.02	1.69	1.74	2.00	1.60	1.50	2.80	1.60	2.20
Gd	5.9	4.9	5.2	4.7	–		–	–	–	–
Tb	–	–	–	–	–	1.10	0.65	1.70	0.70	1.10
Dy	–	–	–	–	–	6.1	–	5.6	3.9	–
Ho	–	–	–	–	–	–	–	–	–	–
Er	–	–	–	–	–	–	–	–	–	–
Yb	–	–	–	–	1.80	2.10	1.00	1.50	2.00	1.70
Lu	1.63	1.52	2.01	1.63	0.30	0.30	0.14	0.10	0.30	0.24

Table 3. (Contd.)

Component	Southeastern sector									
	Ile des Cendres						Dalat			
	11	12	13	14	15	16	17	18	19	20
	9	10-7b	19b	32-7	32-8	35-8	711-20	711-25	736-42	B-10
SiO_2	48.40	46.90	47.68	44.44	47.88	46.92	47.94	52.27	51.47	52.10
TiO_2	2.36	2.20	2.20	2.36	1.97	2.89	1.62	2.48	1.79	1.66
Al_2O_3	15.76	15.54	15.17	12.20	11.94	14.56	14.26	15.79	14.12	16.71
Fe_2O_3	1.85	3.25	2.67	4.90	4.27	1.66	4.80	5.06	–	5.70
FeO	9.45	9.25	9.77	6.38	7.64	9.65	6.92	5.52	10.28	5.07
MnO	0.13	0.15	0.11	0.17	0.17	0.15	0.17	0.30	0.14	0.14
MgO	6.20	6.56	6.35	9.30	10.26	7.80	8.19	5.59	7.24	3.63
CaO	6.91	8.12	7.81	9.96	9.46	7.28	8.65	7.58	9.06	6.23
Na_2O	4.38	4.13	4.60	4.60	3.25	4.05	2.56	2.95	2.56	4.00
K_2O	2.98	2.93	2.93	1.90	1.80	3.05	0.56	2.45	0.28	2.60
P_2O_5	0.45	0.52	0.40	0.60	0.10	1.20	0.27	0.75	0.22	0.35
LOI	0.53	0.08	0.00	2.25	1.00	0.30	4.39	0.00	1.94	2.14
Total	99.40	99.63	99.69	99.06	99.74	99.51	100.33	100.74	99.10	100.33
Sc	–	–	–	–	–	–	–	–	21.4	–
Cr	–	–	256	–	–	–	–	–	225	–
Ni	–	–	86	–	–	–	–	–	187	–
Rb	75	71	69	35	34	71	4.5	40	8	48
Sr	850	840	830	540	510	800	370	540	285	860
Ba	810	1900	800	370	560	230	220	670	208	1500
Hf	7.20	5.20	5.10	5.40	5.20	6.50	2.70	6.90	3.80	6.80
Zr	310	310	290	170	160	300	120	350	110	310
Y	29.0	28.0	25.0	22.0	22.0	27.0	20.0	23.0	22.0	22.0
Ta	4.10	3.20	3.20	2.50	2.10	2.50	1.10	3.40	1.10	3.00
Nb	67	60	60	40	32	64	17	51	18	66
Th	4.30	5.20	5.40	2.10	1.80	2.00	1.80	6.20	1.60	6.50
U	–	–	3.10	–	–	–	–	–	1.10	–
La	55.0	47.0	48.0	27.0	24.0	52.0	15.0	40.0	10.9	43.0
Ce	100	100	98	51	48	98	33	81	24.2	84
Pr	–	–	–	–	–	–	–	–	–	–
Nd	43.0	42.0	41.0	24.0	23.0	42.0	18.0	39.0	14.3	39.0
Sm	8.1	7.8	7.8	5.1	4.8	7.9	4.3	7.8	4.2	8.3
Eu	1.90	2.40	2.40	1.30	1.60	2.20	1.40	2.20	1.50	2.80
Gd	–	–	–	–	–	–	–	–	–	–
Tb	1.10	1.10	1.10	0.81	0.89	1.00	0.80	1.10	0.80	1.20
Dy	–	–	–	–	–	–	–	–	3.3	–
Ho	–	–	–	–	–	–	–	–	–	–
Er	–	–	–	–	–	–	–	–	–	–
Yb	2.20	1.90	1.90	1.60	1.80	2.00	1.60	1.80	1.70	1.40
Lu	0.34	0.27	0.28	0.24	0.27	0.29	0.24	0.26	0.20	0.20

Table 3. (Contd.)

Component	Southeastern sector								Southwestern sector	
	Xuan Loc						Thu Island		Phuoc Long	
	21	22	23	24	25	26	27	28	29	30
	507-29	507-31	507-32	SL-1	507-30	507-6	O34-3	O3416	804178	PL-1
SiO_2	41.02	40.80	41.98	57.58	47.98	40.44	48.56	50.44	50.54	49.16
TiO_2	3.41	2.62	3.19	1.02	1.86	3.73	2.05	2.28	1.88	2.49
Al_2O_3	12.15	12.13	12.29	17.99	13.99	14.90	13.61	14.65	14.80	14.49
Fe_2O_3	6.07	3.84	4.80	–	4.09	8.61	2.67	8.23	–	–
FeO	6.42	10.68	7.45	5.74	7.20	6.14	9.14	4.11	10.53	11.45
MnO	0.13	0.26	0.16	0.11	0.36	0.17	0.13	0.02	0.22	0.16
MgO	10.72	12.04	10.74	3.18	7.36	7.92	9.50	5.84	6.82	7.33
CaO	10.10	9.70	9.80	3.37	9.38	9.29	8.79	7.10	9.01	7.84
Na_2O	1.80	3.17	2.55	6.12	2.65	1.26	2.70	3.24	2.76	3.01
K_2O	1.58	0.72	1.68	4.69	0.87	0.62	1.76	1.82	0.36	1.67
P_2O_5	0.48	0.53	0.46	0.68	0.36	0.60	0.16	0.43	0.28	0.51
LOI	5.80	3.37	4.41	0.34	4.52	5.80	1.18	2.26	2.21	1.66
Total	99.68	99.86	99.51	100.82	100.62	99.48	100.25	100.42	99.41	99.77
Sc	–	–	–	6.3	–	–	–	–	22.1	16.8
Cr	–	313	324	45	–	259	–	–	204	134
Ni	–	296	293	54	–	295	–	–	161	135
Rb	84	85	107	102	4.9	22	40	12	7	33
Sr	820	903	689	1307	370	774	670	740	334	503
Ba	990	899	831	352	620	740	1400	660	79	422
Hf	6.50	7.40	7.50	12.90	5.80	9.00	5.90	6.10	3.70	4.40
Zr	300	310	243	619	160	249	190	260	129	188
Y	25.0	32.0	26.0	26.0	22.0	20.0	28.0	33.0	24.0	29.0
Ta	2.40	–	–	4.00	2.10	–	2.50	2.40	1.50	2.40
Nb	70	69	67	115	19	65	36	51	22	38
Th	1.80	7.60	7.20	16.00	1.50	8.40	2.30	2.80	1.70	4.00
U	–	1.80	1.50	–	–	1.20	–	–	0.30	0.90
La	46.0	57.6	60.5	88.4	15.0	66.1	32.0	43.0	13.7	29.4
Ce	98	107	110	136.1	33	124	62	88	30.1	56.5
Pr	–	13.4	13.1	–	–	16	–	–	–	–
Nd	42.0	51.9	51.7	59.1	19.0	60.0	32.0	42.0	16.0	28.8
Sm	8.3	8.7	9.2	10.7	4.9	11.4	6.7	9.3	4.4	6.7
Eu	2.50	2.94	2.96	1.20	1.70	3.57	2.00	2.60	1.50	2.10
Gd	–	7.6	8	–	–	10.8	–	–	–	–
Tb	1.10	–	–	–	0.97	–	1.10	1.30	1.10	1.10
Dy	–	6	5.9	–	–	8.4	–	–	3.8	5.6
Ho	–	0.97	0.96	–	–	1.37	–	–	–	–
Er	–	2.4	2.5	–	–	3.2	–	–	–	–
Yb	1.60	1.70	1.70	2.80	1.50	2.30	1.90	2.20	1.70	1.60
Lu	0.23	0.17	0.12	0.30	0.22	0.28	0.26	0.31	0.20	0.20

Note: Analyses (1)–(4) are cocites; (6), (9), (19), and (29) quartz tholeiites; (5), (17), (27), and (30) olivine tholeiites; (7), (8), (10), (11), (13)–(16), (18), and (28) alkali olivine basalts; (12) and (21)–(23) basanites; (25) and (26) hawaiites; (20) trachybasalt; and (24) trachyandesite. Analyses (1)–(4) are after Polyakov *et al.* (1997); (5), (6), (9), (24), (29), and (30) are after Hoang *et al.* (1996).

within 1.7–2.2 and 3.9–7.0 in the *Qtz* tholeiites and within 2.6–3.5 and 11.5–19.3 in the *Ol* tholeiites, respectively. The *Qtz* tholeiites show high $^{87}Sr/^{86}Sr$ (0.705121–0.705851) and low $^{143}Nd/^{144}Nd$ (0.512731–0.512786) ratios, and the *Ol* tholeiites have more depleted characteristics ($^{87}Sr/^{86}Sr$ = 0.70414–0.704969 and $^{143}Nd/^{144}Nd$ = 0.512715–0.51286; Fig. 5a). The $^{206}Pb/^{204}Pb$ values of these rocks are similar at 18.34–18.89 (Fig. 6; Hoang *et al.*, 1996).

The upper complex has an age of 0.6–2.5 Ma (Novikov *et al.*, 1989; Hoang *et al.*, 1998) and is composed of flows of alkali olivine basalts and minor mugearites. With respect to silica–alkali relationships, the basaltoids are mildly alkaline. The rocks are rich in TiO_2 (2.2–2.8 wt %), P_2O_5 (0.5–1.0 wt %), and incompatible trace elements (Fig. 3p), including the light REE (La_n/Sm_n = 3.7–3.9 and La_n/Yb_n = 26.2–27.1). In the Th–Hf–Ta diagram (Fig. 4b), the alkali basalts plot together with tholeiites within the WPB field. With respect to isotopic compositions (Figs. 5a, 6), the alkali basalt of the upper complex is similar to the *Ol* tholeiites of the lower complex ($^{87}Sr/^{86}Sr$ = 0.7045, $^{143}Nd/^{144}Nd$ = 0.512849, and $^{206}Pb/^{204}Pb$ = 18.840; Hoang *et al.*, 1996).

The Buon Ma Thuot area is made up of *Ol* tholeiites and alkali basaltoids. However, in contrast to other volcanic areas of Vietnam, alkaline volcanics occur in the lower complex (3.3–4.6 Ma) and tholeiites, in the upper complex (0.3–1.9 Ma) (Hoang *et al.*, 1998). The geochemical characteristics of the alkali basalts and tholeiites of Buon Ma Thuot (Fig. 3q) are similar to those of Pleiku rocks, except for the smaller degree of LREE enrichment (La_n/Sm_n is 2.9–3.7 and 2.6–4.3, and La_n/Yb_n is 14.5–19.5 and 12.7–20.5, respectively). The isotopic characteristics of the alkali basalts and tholeiites are similar to each other, and they are more depleted that the respective rocks from the Pleiku area ($^{87}Sr/^{86}Sr$ = 0.703831–0.703935, $^{143}Nd/^{144}Nd$ = 0.512833–0.512927, and $^{206}Pb/^{204}Pb$ = 18.28–18.66) (Figs. 5a, 6; Hoang *et al.*, 1996).

The Quang Ngai/Re Islands contain a similar association of *Qtz*-normative tholeiites and alkali basalts. The tholeiites of the lower complex (12 Ma) and the alkali basalts of the upper complex (0.4–1.2 Ma) (Hoang *et al.*, 1998) show intraplate-type trace element distribution patterns (Fig. 3k). Their isotopic compositions are variable (Figs. 5a, 6). The tholeiite of the Quang Ngai/Re Islands displays a weakly depleted signature ($^{87}Sr/^{86}Sr$ = 0.704019, $^{143}Nd/^{144}Nd$ = 0.51287, and $^{206}Pb/^{204}Pb$ = 18.57), whereas two alkali olivine basalts have strongly different isotopic characteristics ($^{87}Sr/^{86}Sr$ of 0.704028 and 0.706085, $^{143}Nd/^{144}Nd$ of 0.512831 and 0.512635, and $^{206}Pb/^{204}Pb$ of 18.47 and 18.68; Hoang *et al.*, 1996).

A similar association of tholeiites and alkali olivine basalts of Pliocene–Early Quaternary age (Novikov *et al.*, 1989) was also found in the coast of the South China Sea, where thin lava sheets occur in the Batagan Peninsula and the Song Cau area (Fig. 1). The isotopic composition of the alkali olivine basalt ($^{87}Sr/^{86}Sr$ = 0.704957, $^{143}Nd/^{144}Nd$ = 0.512853, and $^{206}Pb/^{204}Pb$ = 18.65) is similar to that of the Pleiku basalts (Figs. 5a, 6).

The southeastern sector comprises both the oldest (Dalat) and the youngest (Xuan Loc) volcanic centers confined to northeast-trending strike-slip faults and grabens, and a number of volcanic islands (Thu and Katuik) in the shelf zone of the South China Sea (Fig. 1).

Numerous basaltic flows form a large volcanic plateau in the Dalat area. Its lower part (10.5–22.5 Ma; Lee *et al.*, 1998) is dominated by *Qtz* tholeiites and contains minor low-titanium *Ol* tholeiites, and the upper part is composed of *Ol* tholeiite flows (1.8–2.6 Ma) and rare flows of basanite, trachybasalt, trachyandesite, and trachyte (<1.8 Ma).

The quartz tholeiites of the lower complex are distinguished by low alkalinity and high TiO_2 contents (1.75–2.2 wt %). The rocks are slightly enriched in HFSE relative to LILE (Fig. 3r). Their spider diagrams display no Ta–Nb minimum, and sometimes there is an enrichment in these elements. In the Th–Hf–Ta diagram (Fig. 4b), the tholeiites plot within the E-MORB field. The REE distribution patterns are weakly fractionated (La_n/Sm_n = 1.6–2.5 and La_n/Yb_n = 2.3–8.0). The tholeiites have moderately depleted initial isotopic ratios: $^{143}Nd/^{144}Nd$ = 0.512813–0.512882, $^{206}Pb/^{204}Pb$ = 18.01–18.71 (Hoang *et al.*, 1996), and $^{87}Sr/^{86}Sr$ = 0.703822–0.704135 (Figs. 5a, 6).

Compared with the rocks of the lower complex, the *Ol* tholeiites of the upper complex are more alkaline (at the expense of potassium) and show higher phosphorus at similar titanium concentrations. The volcanics are more enriched in incompatible elements, first of all, in LILE and Nb (Fig. 3r). Less common basanites are strongly enriched in both LILE and HFSE and plot within the WPB field in the Th–Hf–Ta discriminant diagram (Fig. 4b). The alkaline basaltoids show strongly fractionated REE distribution patterns with strongly enriched light REE (La_n/Sm_n = 3.2 and La_n/Yb_n = 20.2). The trachyandesites and trachytes are characterized by medium (similar to trachybasalts) alkali contents and low concentrations of P, Sr, and Ba. The rocks usually have a strong Nb minimum (Fig. 3r).

Another occurrence of basaltoids in the southeastern sector of Vietnam is the Xuan Loc area, where two episodes of volcanic activity were also documented. Its lower (2.2–2.42 Ma) complex is composed of *Ol* tholeiite flows, and the upper complex (0.4–1.1 Ma; Lee *et al.*, 1998) is made up of flows of alkali olivine basalts, basanites, and occasional trachyandesites and basanitic scoria cones. The tholeiites are characterized by low aluminum, sodium, and LILE and high HFSE contents. There is no Ta–Nb depletion, and a positive anomaly in these elements may occur (Fig. 3u). In the Th–Hf–Ta diagram (Fig. 4b), the tholeiites plot within the E-MORB field. The isotopic characteristics of the *Ol* tholeiites vary from slightly depleted to OIB-like:

$^{87}Sr/^{86}Sr$ = 0.703686–0.704807, $^{143}Nd/^{144}Nd$ = 0.512716–0.512886, and $^{206}Pb/^{204}Pb$ = 18.24–18.32 (Figs. 5a, 6). The basaltoids of the upper complex are moderately alkaline olivine basalts and basanites. The basanites are strongly enriched in HFSE and LILE (Fig. 3u) and fall within the WPB field in the Th–Hf–Ta diagram (Fig. 4b). The rocks show fractionated REE distribution patterns with strongly enriched light REE (La_n/Sm_n = 2–7 and La_n/Yb_n = 7–24). The isotopic ratios of the alkaline basaltoids vary slightly and are similar to those of OIB: $^{87}Sr/^{86}Sr$ = 0.704117–0.704348, $^{143}Nd/^{144}Nd$ = 0.512773–0.512853, and $^{206}Pb/^{204}Pb$ = 18.12–18.32 (Figs. 5a, 6). The trachyandesites show high alkali and aluminum contents, strong enrichment in incompatible elements (Fig. 3u), and fractionated REE distribution patterns (La_n/Sm_n = 5 and La_n/Yb_n = 20.8). The strontium isotope composition of the trachyandesites is more enriched than that of the alkali basalts ($^{87}Sr/^{86}Sr$ = 0.704807), although these rocks have similar $^{143}Nd/^{144}Nd$ = 0.512716 and $^{206}Pb/^{204}Pb$ = 18.24 (Figs. 5a, 6).

The Pleistocene scoria cones of Thu Island are built up of hawaiites and occasional mugearites (Koloskov, 1999). The rocks are low aluminous and moderately alkaline ($Na_2O + K_2O$ = 5.0–5.2 wt %) with a high fraction of potassium (K_2O/Na_2O = 0.55–0.65). The concentrations of all incompatible elements are high (Fig. 3v) and approach those of intraplate basalts, which is in line with the low Th/Ta ratios, the distribution of hawaiite points in the Th–Hf–Ta diagram (Fig. 4b), and the fractionated REE distribution patterns (La_n/Sm_n = 2.7–2.9 and La_n/Yb_n = 11.1–14.5).

The middle Pleistocene–Recent (from 0.8 Ma to historic eruptions) volcanic edifices of Ile des Cendres Volcano in the Katuik archipelago are composed of pyroxene–olivine–plagioclase basalts. With respect to silica–alkali relationships, the basalts belong to the alkaline series ($Na_2O + K_2O$ = 5.4–7.4 wt %); they show high concentrations of aluminum, titanium (2.0–2.9 wt % TiO_2), and phosphorus (0.5–1.2 wt % P_2O_5), and low magnesium (Table 3). The abundances of transitional elements vary slightly: 190–320 ppm Cr and 180–90 ppm Ni. The concentrations of incompatible elements are high (Fig. 3w), and there is either a small enrichment or no anomaly in Ta and Nb. In the Th–Hf–Ta diagram (Fig. 4b), the most alkaline basalts of Ile des Cendres Volcano fall within the WPB field, whereas less alkaline varieties approach the E-MORB field. Their REE distribution patterns are fractionated with a strong LREE enrichment (La_n/Sm_n = 2.8–4.2 and La_n/Yb_n = 8.8–22.5). The initial strontium and neodymium isotope ratios in two samples vary within 0.704861–0.705318 and 0.512708–0.512754 (Fig. 5a), respectively, and their $^{206}Pb/^{204}Pb$ ratio (18.19) is also moderately depleted (Fig. 6).

It is noteworthy that some basalts from Ile des Cedres Volcano carry disintegrated and strongly reworked quartz–feldspar and granitoid xenoliths and relics of resorbed quartz grains (Koloskov, 1999).

The southwestern sector of Vietnam comprises the eastern portion of the Khorat Plateau, which is made up of Precambrian basement rocks and surrounded by Paleozoic and Mesozoic terrains (Tung and Tri, 1992). The largest volcanic area of Indochina, Phouc Long, is situated in this sector. It is about 200 km long and has a total thickness of up to 500 m (Hoang *et al.*, 1998). This area includes two basaltic complexes.

The lower complex (15.0–15.1 Ma; Lee *et al.*, 1998) consists of *Qtz*-normative and occasional *Ol*-normative tholeiites. The clinopyroxene–plagioclase *Qtz* tholeiites show high silica and low alkali ($Na_2O + K_2O$ = 3.1–4.0 wt %) and phosphorus contents (0.18–0.28 wt % P_2O_5). The rocks usually have slightly varying concentrations of transitional elements (160–230 ppm Cr, 120–170 ppm Ni, and 19–22 ppm Sc), and low concentrations of LILE and HFSE. The *Qtz* tholeiites display a distinct Ta–Nb maximum on spider diagrams (Fig. 3s) and variable Ta contents (0.8–1.6 ppm). This results in that the points of tholeiites are widely scattered over the E-MORB and WPB fields in the Th–Hf–Ta diagram (Fig. 4b). Their REE distribution patterns are weakly fractionated (La_n/Sm_n = 1.3–2.1 and La_n/Yb_n = 3.2–6.7). The quartz tholeiites of the Phouc Long area show slightly depleted compositions with $^{87}Sr/^{86}Sr$ = 0.70356–0.704294, $^{143}Nd/^{144}Nd$ = 0.512864–0.512922, and $^{206}Pb/^{204}Pb$ = 18.57–18.67 (Figs. 5a, 6).

The olivine–clinopyroxene–plagioclase basalts of the upper complex (~5 Ma) are *Ol*-normative tholeiites differing from the tholeiites of the lower complex in lower silica and higher alkali (at the expense of higher potassium), magnesium, titanium, and phosphorus contents. They usually show higher incompatible element concentrations and more fractionated REE distribution patterns (La_n/Sm_n = 2.6–2.9 and La_n/Yb_n = 12–14). In the Th–Hf–Ta diagram (Fig. 4b), the points of *Ol* tholeiites occur within the WPB field. The isotopic characteristics of tholeiites from the upper and lower complexes are similar: $^{87}Sr/^{86}Sr$ = 0.703832–0.703917, $^{143}Nd/^{144}Nd$ = 0.512859–0.512878, and $^{206}Pb/^{204}Pb$ = 18.45–18.53 (Figs. 5a, 6).

The southern Khorat Plateau in Thailand contains a number of small sheets of alkaline basaltoids and tholeiites of early Pleistocene age (Fig. 1; Zhou and Mukasa, 1997). Two groups with different chemical and isotopic characteristics (Table 4) were distinguished among the basalts (Zhou and Mukasa, 1997). The first group includes the alkali olivine basalts, hawaiites, and *Ol* tholeiites of the Nakhon Ratchasima and Phu Naonan areas, and the second group includes a number of small alkali olivine basalt, hawaiite, and trachybasalt sheets between the towns of Khorat and Sisaket (Surion, Prai Bat, and other areas; Fig. 1).

The basaltoids of the first group show lower SiO_2 and higher iron oxide and CaO concentrations. They are characterized by strongly variable distribution pat-

Table 4. Representative analyses of Cenozoic volcanics from Thailand (Mukasa *et al.*, 1996; Zhou and Mukasa, 1997)

Component	Bo Floi*	Denchai			Chanthaburi	Nakhon Ratchasima		Phu Naoan	Surion	Prai Bat
	1	2	3	4	5	6	7	8	9	10
	ABP4**	ADC1	ADC-8	ADC-3	Bkpw3	NR-10	NR-11	PNG3	SR-27	BY-29
SiO_2	46.28	46.79	49.02	52.14	41.35	49.69	47.52	43.62	52.60	52.69
TiO_2	1.93	2.34	2.09	1.85	3.01	2.41	2.54	2.36	2.31	2.74
Al_2O_3	16.41	16.66	19.22	17.29	11.87	15.95	14.61	13.49	14.79	15.05
Fe_2O_3	1.28	1.38	1.13	1.07	1.72	–	–	–	–	–
FeO	8.55	9.17	7.56	7.16	11.50	11.66	12.56	12.51	8.67	9.03
MnO	0.17	0.16	0.14	0.12	0.18	0.15	0.16	0.18	0.10	0.12
MgO	6.99	8.57	4.59	5.72	12.16	3.39	5.88	6.46	5.96	4.74
CaO	8.32	8.81	5.92	7.27	9.55	7.70	8.47	9.52	6.09	7.48
Na_2O	4.56	3.08	5.27	3.17	4.04	3.12	3.40	4.77	4.07	3.88
K_2O	3.52	2.35	1.62	2.60	1.41	1.58	1.93	2.13	1.78	1.53
P_2O_5	0.95	0.69	0.87	0.58	1.21	0.52	0.73	1.62	0.74	0.79
LOI	0.00	0.00	0.00	0.00	0.00	0.00	0.00	0.00	0.00	0.00
Total	98.96	100.00	97.43	98.97	98.00	96.17	97.80	96.66	97.11	98.05
Sc	–	–	–	–	–	18.1	17.4	11.3	11.4	12.5
Cr	–	–	–	–	–	216.1	244	102.4	120.5	131.7
Ni	126.8	151.1	42.4	91.7	7	182.8	189.7	120.4	73.1	150
Co	37	45	28	36	60	48.7	54.3	45.9	29	39.9
Rb	168.9	36.7	43	45.5	33.8	14.1	23	42.6	26.8	17.3
Sr	1124.2	765.7	862.4	619	1152.3	569.8	741.6	1385.5	718.6	915.2
Ba	529	423	599	520	789	590.7	568.6	557.7	352.2	372.3
Hf	6.20	4.70	5.70	4.20	6.60	4.40	5.00	5.20	5.70	5.60
Zr	290.2	218.2	285.5	191.8	303	157.3	179.4	179.5	201.8	207.6
Y	26.8	23.5	21.7	22.8	28.9	45.1	21.8	25.0	18.4	20.8
Ta	6.30	2.90	3.80	2.60	4.90	2.10	2.70	5.30	2.00	1.80
Nb	115.3	64.5	72.8	46	97.3	29.9	37.1	71.6	26.3	25.7
Th	15.00	4.30	6.20	5.00	9.20	2.60	3.90	8.90	2.20	1.90
U	–	–	–	–	–	0.50	1.20	1.30	0.50	0.50
La	65.0	31.0	39.0	27.0	65.0	38.6	21.6	77.4	27.0	23.9
Ce	109	57	70	53	119	58.5	63.9	152.1	55.4	61.9
Nd	48.0	27.0	38.0	32.0	55.0	53.5	31.3	64.8	36.7	40.8
Sm	8.7	6.4	6.1	5.6	10.8	12.8	7.4	12.9	8.7	10.1
Eu	2.70	2.00	1.90	1.60	3.40	4.00	2.60	4.10	2.70	2.90
Tb	0.70	1.30	0.60	0.90	1.40	1.40	1.10	1.50	1.00	1.10
Dy	2.7	4.8	4	3.8	5.2	–	–	–	–	–
Yb	2.30	2.10	1.90	2.10	1.80	2.40	1.40	1.40	1.10	1.20
Lu	0.30	0.30	0.30	0.30	0.20	0.30	0.10	0.10	0.10	0.10

Note: Analyses (1), (2), and (5) are basanites; (3) and (8) hawaiites; (4) mugearite; (6) and (7) olivine tholeiites; (9) and (10) trachybasalts.

terns of incompatible elements, persistent Ta and Nb enrichment, and relative depletion in Zr and Hf (Fig. 3m). In the Th–Hf–Ta diagram (Fig. 4d), the majority of these basaltoids plot within the WPB field. Their REE distribution patterns are fractionated. The degree of enrichment in the light lanthanides change considerably from the olivine tholeiites (La_n/Sm_n = 1.3–1.8 and La_n/Yb_n = 4–10) to alkali basalts (La_n/Sm_n = 2.2–3.7

and La_n/Yb_n = 12–55). The rocks of various groups show similar isotopic characteristics and are slightly depleted in radiogenic isotopes: $^{87}Sr/^{86}Sr$ = 0.70354–0.70384, $^{143}Nd/^{144}Nd$ = 0.51286–0.51295, and $^{206}Pb/^{204}Pb$ = 18.22–18.46 (Figs. 5a, 6).

With respect to incompatible element distribution, the basalts of the second group are very uniform (Zhou and Mukasa, 1997) and resemble intraplate alkali basalts (Sun and McDonough, 1989). However, their points tend toward the E-MORB field in the Th–Hf–Ta diagram (Fig. 4d). Their REE distribution patterns are fractionated (La_n/Sm_n = 1.2–2.1 and La_n/Yb_n = 8–28) but to a smaller extent compared with the basaltoids of the first group. The isotopic signatures of the two basalt groups are strongly different. The basalts of the second group show lower $^{143}Nd/^{144}Nd$ = 0.51266–0.51281, higher $^{87}Sr/^{86}Sr$ = 0.70486–0.70585 and $^{206}Pb/^{204}Pb$ = 18.49–18.65, and more heterogeneous isotopic compositions.

West of the Khorat Plateau, Cenozoic volcanism occurred in two tectonic zones (terrains): Shan Thai (Bo Phloi area) and eastern Indochina (Denchai, Lop Buri, Chanthaburi, and Tha Mae areas) divided by the Nan suture.

The Cenozoic volcanics of the Shan Thai zone form small necks and isolated lava flows over an area of 0.5 km^2 in the field of Silurian–Devonian metamorphic rocks. The Bo Phloi volcanic area (Fig. 1) is dominated by basanites and nepheline hawaiites. The K–Ar age of these volcanics was estimated as 3.15 ± 0.17 Ma (Barr and Macdonald, 1981). According to Mukasa *et al.* (1996), the rocks are rich in alkalis ($Na_2O + K_2O$ = 6.7–8.9 wt %), phosphorus, and aluminum, and have moderately high titanium contents (Table 4). The abundances of all incompatible elements are high (Fig. 3m) and approach those of intraplate alkali basalts. There is a persistent enrichment in Ta and Th, which shifts the points of these rocks in the Th–Hf–Ta diagram into the region between the active continental margin and intraplate basalt fields (Fig. 4d). The REE distribution patterns are fractionated with a strong enrichment in the light lanthanides (La_n/Sm_n = 4.5–4.6 and La_n/Yb_n = 18–21). The $^{87}Sr/^{86}Sr$ ratios of the Bo Phloi basaltoids are somewhat depleted relative to the BSE (0.70381–0.704255); however, they show low $^{143}Nd/^{144}Nd$ (0.51273–0.51285) and high $^{206}Pb/^{204}Pb$ values (18.42–18.62) (Mukasa *et al.*, 1996).

The Denchai area with an age of 5.62–6.06 Ma (Barr and Macdonald, 1981) is situated in the northern part of the Central Thai graben (Fig. 1) and comprises a series of thin flows composed of two parts: lower hawaiite and upper hawaiite and basanite. These basaltoids differ from the Bo Phloi rocks in more variable silica contents, lower alkalis ($Na_2O + K_2O$ = 5.4–6.9 wt %), lower phosphorus, and higher titanium and nickel contents. Similar to the Bo Phloi basaltoids, their incompatible element distribution patterns (Fig. 3m) resemble those of WPB, which is additionally supported by the position of these rocks in the Th–Hf–Ta diagram (Fig. 4d). They are usually less enriched in the light REE (La_n/Sm_n = 2.9–3.9 and La_n/Yb_n = 8.5–13.5). The isotopic ratios of the basalts are strongly variable: $^{87}Sr/^{86}Sr$ = 0.70375–0.7043, $^{143}Nd/^{144}Nd$ = 0.51280–0.51293, and $^{206}Pb/^{204}Pb$ = 18.24–18.72.

The Pleistocene (0.44 ± 0.11 Ma; Barr and Macdonald, 1981) areas of Chanthaburi and Tha Mae are situated in the southeastern flank of the Central Thai graben (Fig. 1) and are also made up of basanite and nephelinite flows. According to Mukasa *et al.* (1996), the Chanthaburi basaltoids are assigned to the alkaline series and show high concentrations of magnesium, titanium (3.0–3.3 wt % TiO_2), phosphorus (1.1–1.4 wt % P_2O_5), and Ni (160–320 ppm) and low aluminum (Table 4). Compared with other basaltoids of Indochina, these rocks have the maximum enrichment in incompatible elements (Fig. 3m) and high La_n/Sm_n (3.5–3.7) and La_n/Yb_n (23.5–23.7). In the Th–Hf–Ta diagram (Fig. 4d), the compositions of alkali basalts from the Chanthaburi area plot within the WPB field. The isotopic compositions of the Chanthaburi basaltoids are slightly depleted relative to the BSE: $^{87}Sr/^{86}Sr$ = 0.70387–0.70431, $^{143}Nd/^{144}Nd$ = 0.51286–0.51290, and $^{206}Pb/^{204}Pb$ = 18.39–18.64 (Mukasa *et al.*, 1996).

CORRELATION OF CENOZOIC MAGMATIC AND GEODYNAMIC EVENTS IN THE SOUTH CHINA AND INDOCHINA REGIONS

Overstresses related to the India–Eurasia collision (Tapponnier *et al.*, 1986) promoted the appearance of northeast-trending extensional zones, along which rift structures were initiated (Ru and Piggott, 1986) and volcanic complexes were formed. A change in the thermal structure of the lithosphere in the late Paleocene–Eocene caused its heating and melting and was responsible for the formation of shoshonitic and high-potassium magnesian lavas in the Tibet (Turner *et al.*, 1996), Yunnan province of China (Zhu *et al.*, 1992), and northern Vietnam (Hoa *et al.*, 1995; Polyakov *et al.*, 1997; Fig. 4a). The opening of the South China Sea (32–17 Ma) after the collision between India and Eurasia began in the Paleogene from extensional detachment processes in the continental margin (Briais *et al.*, 1989). The formation of pull-apart basins and spreading of the South China Sea resulted in the disintegration of the margin and separation of crustal blocks, whose fragments are now represented by the Paracel and Dongsha islands, Reed and Macclesfield banks, Dangerous Grounds, and North Palawan continental terrain (Tu *et al.*, 1992). In southeastern China, the Paleocene–Eocene extensional processes led to the formation of rift depressions in the Guangdong province and areas of bimodal basalt–trachyte volcanism. Some basalts of these areas inherited subduction signatures (Chung *et al.*, 1997). In the Oligocene the stage of graben formation and rifting in the South China Sea gave way to a spreading process, which resulted in

the separation of the southwestern and eastern parts of the deep marine basin.

In the earliest Miocene, the northwestward propagation of extensional zones resulted in the thinning of the lithosphere and asthenosphere upwelling. The axis of rifting lay along the western part of the Taiwan Strait (Angelier *et al.*, 1990; Chung *et al.*, 1994, 1995; Zou *et al.*, 2000). These events caused the establishment of a rift regime in the Fujian–Taiwan region. In the early Miocene, intraplate alkali basalts of the Kungkuan complex were formed in northwestern Taiwan. Their isotopic ratios are shifted toward the EMII field. They were replaced in the late middle and late Miocene by alkali basalts and tholeiites formed under the influence of the EMI component (Chung *et al.*, 1995). The earliest volcanic activity of the Fujian province occurred in the outer zone, and its maximum development was recorded in all zones in the middle–late Miocene. Volcanism in the inner zone persisted up to the late Quaternary. The dominant types of volcanics change from the outer to the inner zone from olivine tholeiite, through alkali olivine basalt, to basanite and nephelinite. The Sr–Nd–Pb isotopic systematics of these volcanics suggest a contribution from the EMII source to their genesis and indicate an influence of the DUPAL anomaly (Zou *et al.*, 2000). In the middle Miocene, tholeiitic basalt volcanism occurred in the Scarborough seamounts of the South China Sea. It surrounded an extinct spreading zone and replaced it with intraplate tholeiites, which changed to intraplate alkaline compositions in the late Miocene–early Pliocene (Tu *et al.*, 1992). In the Indochina region, Miocene volcanism is known in the Dalat and Phouc Long areas and the Quang Ngai/Re Islands, where *Qtz* tholeiites and minor *Ol* tholeiites were formed, and in the northern part of the Central Thai graben, where late Miocene alkaline magmatism produced series of flows with hawaiites in the lower parts and hawaiites and basanites in the upper parts (Mukasa *et al.*, 1996).

The Pliocene–Quaternary stage of volcanism was widespread both in the southern China and Indochina regions. In southeastern China, in addition to intense alkali basalt volcanism in the central and inner zones of the Fujian province, basaltic volcanism occurred in the Leizhou Peninsula and Hainan Island. The lower complexes of both areas consist of intercalating *Qtz* and *Ol* tholeiite flows with intraplate geochemical characteristics and without suprasubduction isotopic signatures. Scoria cones and central-type volcanic edifices of the upper complex are made up of alkaline basaltoids. In the South China Sea region, the volcanic structures of the Paracel Islands developed at that time. They are dominated by nephelinites with significantly lower Pb isotope ratios and higher $^{143}Nd/^{144}Nd$ compared with the alkaline basaltoids of the Scarborough seamounts. Intense basaltic volcanism in the Reed Bank seamounts produced alternating olivine basalts and olivine tholeiites (Tu *et al.*, 1992). The middle Pleistocene–Holocene volcanism of the Okinawa Trough gave rise to bimodal tholeiitic basalt–rhyolite suites (Shinjo *et al.*, 1999). In the Indochina region, Pliocene–Quaternary volcanic occurrences are known in all sectors and are dominated by intraplate tholeiitic or alkaline basaltoids.

PROBABLE SOURCES OF VOLCANISM

The results of our analysis allow us to evaluate main regularities in the development of Cenozoic volcanism in the southeastern margin of the Asian continent and constrain the nature of deep magma sources.

In Cretaceous time extended continental margin volcanic belts were formed in the eastern Asian margin. However, by the middle Early Paleogene, geodynamic conditions changed abruptly: after the seaward displacement of subduction zones and the beginning of collision processes, the Asian continental margin underwent an extensional regime with the formation of a system of normal faults, grabens, transtensional faults, up to marginal marine basins.

The earliest postsubduction volcanic complexes of southeast Asia are represented by three compositional associations: the bimodal tholeiite–trachyte and tholeiite basalt–basaltic andesite associations of the Paleocene–middle Eocene (Chung *et al.*, 1997), the early Oligocene potassic alkaline association in southeastern China (Zhu *et al.*, 1992), and the Oligocene potassic alkaline association of Vietnam (Polyakov *et al.*, 1997; Hoa *et al.*, 1995).

The basalts and basaltic andesites of the tholeiitic series show moderately low HFSE and variably high LILE concentrations, high $^{87}Sr/^{86}Sr$ and low $^{143}Nd/^{144}Nd$ ratios. Together with the negative correlation of $^{143}Nd/^{144}Nd$ and positive correlation of $^{87}Sr/^{86}Sr$ with the concentrations of silica and LILE, these features suggest a significant contribution of crustal material to the genesis of these volcanics (Chung *et al.*, 1997). The negative Ta–Nb anomalies of some basalts and their location in the field of continental margin volcanic series in discriminant diagrams (Fig. 4) make them similar to suprasubduction complexes. However, the confinement of the Heyuan and Lienping volcanics to rift depressions allows us to connect their formation with the early stages of extension in the continental margin.

The Early Paleogene volcanics of the Sanshui area are represented by a bimodal tholeiite–trachyte association, which is distinguished by high HFSE and LILE contents in basic members and considerable enrichment of trachytes. Based on the similarity of tholeiites and trachytes with respect to $^{143}Nd/^{144}Nd$ (0.51268–0.51290 and 0.51279–0.51286, respectively) and a number of element ratios (e.g., Hf/Ta of 2.4–3.8 and 2.1–3.0, Sm/Nd of 0.22–0.27 and 0.20–0.22, Zr/Nb of 5.7–10.8 and 5.1–10.4, respectively), Chung *et al.* (1997) supposed that the rocks of the bimodal association were formed by closed-system differentiation in the lower and upper parts of a magma chamber. The

Table 5. Element ratios in the Cenozoic basalts of Vietnam

Rock	La/Hf	Ta/Yb	Zr/Y	Ba/Sr	Th/Yb	La_n/Yb_n	Hf/Ta	Zr/Nb	K_2O/P_2O_5	Ti/Zr
Qtz tholeiites	2.4–6.8	0.23–1.33	4.1–9.2	0.1–1.3	0.8–3.2	2.3–10.1	2.2–6.2	3.0–7.1	1.3–6.3	0.010–0.017
Ol tholeiites	2.6–7.8	1.28–2.57	4.4–11.3	0.2–1.7	1.0–4.4	6.6–20.5	1.5–2.8	3.2–5.7	0.4–3.9	0.090–0.021
Alkali basalts	3.3–11.3	0.86–4.30	4.6–30.0	0.3–2.3	1.0–7.3	8.2–30.1	1.2–3.2	2.3–6.9	0.3–7.8	0.001–0.063

subsequent crustal contamination of the trachyte melts (1–3%) resulted in an increase in $^{87}Sr/^{86}Sr$ at a constant initial $^{143}Nd/^{144}Nd$ ratio (Chung *et al.*, 1997).

The low-titanium potassic basaltoids (cocites and absarokites) of China and Vietnam show a LILE enrichment relative to HFSE, a distinct negative Ta–Nb anomaly, and low Nb/U ratios (1.5–4.9). On the other hand, in contrast to the rocks of typical suprasubduction series, the Oligocene potassic basaltoids are related to extensional zones, including rift depressions (Shongda in northern Vietnam) and grabens (Haidong in China). It is therefore reasonable to suppose that the potassium-rich basaltoids were formed during the incipient extension of the continental margin, which caused decompression and fractionation of a relatively shallow source in the upper part of the phlogopite-bearing subcontinental lithosphere at very low pressures (<1 GPa) (Barton and Hamilton, 1982; Flower *et al.*, 1998).

Starting from the Miocene, the main volume of volcanics in Southeast Asia (except for the Okinawa Trough and allochthonous ophiolite complexes of the South China Sea) has been represented by enriched olivine and alkali basalts having isotopic and geochemical characteristics similar to those of basaltoids from continental rifts and ocean islands and strongly different from suprasubduction zone volcanics.

The majority of volcanic centers in southeastern China and Indochina were formed by two eruptive complexes, (1) early silica-rich, low-iron, and low-titanium quartz and olivine tholeiites and occasional trachyandesites representing lithospheric mantle sources and (2) late low-silica, high-iron, and high-titanium olivine tholeiites, alkali basalts, basanites, and rare trachybasalts and trachytes connected with asthenospheric mantle sources.

In general, the tholeiites of the region are enriched relative to the primitive mantle and E-MORB-type basalts and are compositionally similar to OIB. There are distinctive features including positive Ba anomalies and low contents of Th, Nb, and Ta. Despite the low concentrations of Ta and Nb, the olivine and quartz tholeiites of the region usually display no Ta–Nb depletion, which is common in similar rocks from a number of localities in the eastern Asian margin (Fedorov *et al.*, 1993, 1999, 2002; Filatova and Fedorov, 2001). A weak negative Ta–Nb anomaly was detected only in the quartz tholeiites of Pleiku. The resemblance of the tholeiites under investigation to the products of intraplate magmatic activity can be observed in a number of diagrams (Figs. 3, 4), where these basalts occur in the E-MORB and WPB fields. The REE characteristics of tholeiites of different ages and from different areas are also similar. The tholeiites show differentiated REE distribution patterns, and the degree of LREE enrichment increases from the *Qtz* tholeiites to *Ol* tholeiites (Fig. 3). The isotopic systematics of the tholeiites suggest that the compositions of rocks range from slightly depleted to moderately enriched relative to the BSE (Fig. 5a).

The alkaline series basaltoids are characterized by moderately high concentrations of alkalis, high titanium and phosphorus, and low aluminum. The concentrations of incompatible elements are high and similar to those of OIB. The alkali basalts of all areas exhibit a minor positive Ta–Nb anomaly, except for the Bao Loc and Xuan Loc basaltic trachyandesites, which show a negative Ta–Nb anomaly. The assignment of the alkaline basaltoids to intraplate complexes is supported by their Th/Ta and Ba/La ratios, the position of points on discriminant diagrams, and the fractionated distribution patterns of incompatible elements (Figs. 3, 4). The basaltoids show smaller variations in lead isotope composition compared with the tholeiites and more variable strontium and neodymium isotope ratios (Fig. 5).

The tholeiites differ from the alkali basalts in lower concentrations of titanium and iron at given MgO. A transition from the quartz tholeiite to alkali basalt is accompanied by an increase in La/Hf, Ta/Yb, Zr/Y, Ba/Sr, Th/Yb, and La_n/Yb_n and a decrease in Hf/Ta, Zr/Nb, K_2O/P_2O_5, and Ti/Zr (Table 5). The olivine tholeiites are transitional between the quartz tholeiites and alkali basalts. According to many authors (e.g., *Large Igneous…*, 1997), such a difference between the tholeiitic and alkali basalts with intraplate geochemical characteristics is most likely related to the heterogeneity of their sources (different depths of melting or entrainment of different zones of the diapir into petrogenetic processes) rather than the character of melting or crystal fractionation and reflects the entrainment of the refractory asthenosphric mantle, enriched lithosphere, or a deep mantle diapir into petrogenesis, which is illustrated by the diagrams of incompatible element distribution (Fig. 3) and isotopic mixing (Fig. 5b).

Chung *et al.* (1994, 1995) explained the zoning of volcanism in the Fujian–Taiwan province of China by suggesting that variations in the depth of melt segregation corresponded to the depth of the lithosphere, which resulted in spatial variability of basalt compositions. The tholeiites of the outer zone of Fujian formed in shallow mantle levels near the axial zone at a relatively

high degree of melting with a dominant contribution of metasomatized material from the enriched asthenosphere (plume). On both sides of the Taiwan Strait, the influence of the plume decreases gradually and the magmas of these zones become more undersaturated and more alkaline owing to an increase in the depth of melt segregation and a decrease in the degree of melting. On the other hand, variations perpendicular to the extension axis in the mixing proportions of materials from the subcontinental lithosphere with prevailing EMII characteristics and a depleted asthenosphere matrix represented by the N-MORB of the East Taiwan ophiolite complex define variations in Pb isotopes and small changes in Sr and Nd isotopic ratios. For instance, the Fujian tholeiites from the outer zone are most enriched in the EMII component, whereas the basanites of the inner zone show the most depleted Pb isotope composition overlapping that of the basalts of the East Taiwan ophiolite complex. The magmas of the Penghu Islands were generated at varying degrees of melting in an area with a relatively steep lithosphere–asthenosphere boundary, which explains the change from olivine tholeiite to alkali basalt composition at relatively constant isotopic characteristics (Chung *et al.*, 1994).

In the Okinawa Trough, the middle Miocene and early Pleistocene nonvolcanic stages of rifting (Kimura, 1985) were followed in the middle Pleistocene–Holocene by bimodal tholeiitic basalt–rhyolite volcanism (Shinjo *et al.*, 1999), which occurred mainly in the middle and, to a lesser extent, in the southern parts of the trough. The Okinawa Trough tholeiites show relatively high concentrations of incompatible elements similar to those of back-arc basalts and OIB-like (PREMA) Sr and Nd isotopic ratios. In addition, they are characterized by the presence of a strong negative Ta–Nb anomaly and element ratios approaching those of suprasubduction volcanics.

A number of researchers have pointed out (Flower *et al.*, 1992; Hoang *et al.*, 1996; Mukasa *et al.*, 1996; Zhou and Mukasa, 1997; Hoang *et al.*, 1998) that, in most cases, crustal contamination did not play a significant role in the compositional variations of basaltoids from the eastern Asian margin. It should also be noted that volcanics from different sectors were formed independently of each other, on different basements, and often at different times. On the other hand, the incompatible element distribution patters of tholeiitic and alkali basalts from various areas are similar within each series, which indicates the similarity of their parental melts. If a significant contribution of crustal material to the genesis of basalt is supposed, it is necessary to determine the mechanism by which crustal material could be added to the initial melts providing uniform compositions of the contaminated products in all the areas (Yarmolyuk *et al.*, 1999), which is improbable. In addition to general considerations, there are certain geochemical constraints on the role of contamination in the genesis of volcanic rocks.

It is known that the addition of a crustal component to basic melt can be accounted for using the positive correlation between $^{87}Sr/^{86}Sr$ and total alkalis, SiO_2, 1/Sr (Fig. 7), Ba/Nb, La/Nb, K_2O/P_2O_5 (Fitton *et al.*, 1988), La/Ta, and Th/Ta (Loubet *et al.*, 1988), although similar relationships could be due to assimilation–fractional crystallization processes or partial melting effects (DePaolo, 1988). Evidence for crustal contamination was found only among the Early Paleogene lavas of south China (Chung *et al.*, 1997) and is practically lacking in younger basalts from this region (Chung *et al.*, 1994; Flower *et al.*, 1992), whereas part of Vietnam basalts and basalts from the southern Khorat Plateau (Thailand) show a positive covariation between $^{87}Sr/^{86}Sr$ and K_2O/P_2O_5. Most of the Vietnam basalts fall within a narrow range of $^{87}Sr/^{86}Sr$ (0.7036–0.7044), and the K_2O/P_2O_5 ratio decreases from the rocks of the lower complex to the upper complex volcanics within each area (Hoang *et al.*, 1996). However, higher values of these ratios were detected in the orthopyroxene-bearing quartz tholeiites of Dien Bien Phu; tholeiites of Xuan Loc, Buon Ma Thuot, and Pleiku; quartz tholeiites of Song Cau; and some alkali basalts from Ile des Cendres submarine volcano. There are two possible approaches to this problem. First, it can be supposed that crustal contamination took part in the genesis of these volcanics. The viability of this mechanism is supported by the presence of abundant quartz–feldspar segregations, quartz grains, and xenoliths of granites and granodiorites with much higher $^{87}Sr/^{86}Sr$ values (Fig. 7). For instance, the compositions of alkali basalts from Ile des Cendres tend toward the EMII component owing to the high $^{87}Sr/^{86}Sr$ values (Fig. 5). This allows us to suppose crustal contamination of the magmas, which is confirmed by the presence of granitoid xenoliths (Koloskov, 1999).

However, the covariations of MgO/FeO_{tot} and $^{87}Sr/^{86}Sr$ are mainly due to melting of a metasomatized (enriched) source rather than direct contamination with crustal material. It should be noted that the increase of the alkali contents and Sr isotopic ratios of rocks is not accompanied by silica enrichment, which also suggests a selective crustal contamination, when low-temperature micas and potassium feldspar are initially resorbed, while quartz remains unassimilated (Koloskov *et al.*, 2003). In addition, the observed differences between the isotopic ratios of basalts from various lithospheric sectors (Zhou and Mukasa, 1997; Hoang and Flower, 1998) suggest that the influence of the enriched mantle prevailed over the processes of crustal contamination, and the majority of volcanic areas of Indochina as well as the whole eastern Asian margin show systematic variations in basaltoid chemistry from the dominance of the EMII component in the tholeiites of the early series to a significant contribution from the EMI component in the alkali basalts of the late series.

In general, the basalts of southeastern Asia show high $^{208}Pb/^{204}Pb$ and $^{207}Pb/^{204}Pb$ ratios and plot above

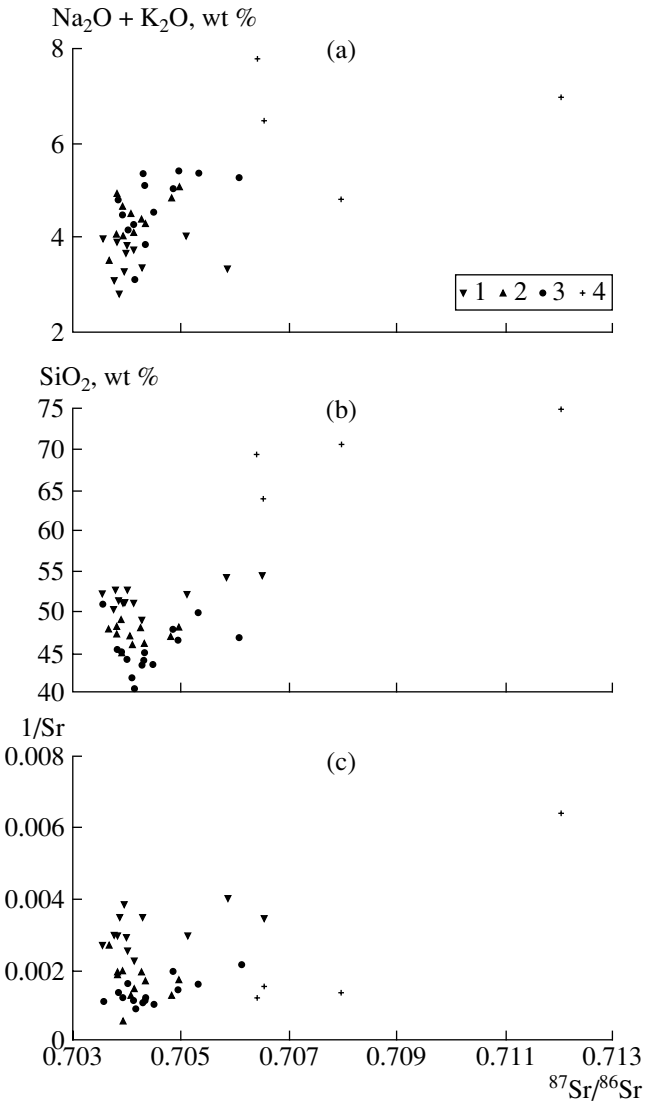

Fig. 7. Variations of $^{87}Sr/^{86}Sr$ as a function of (a) $Na_2O + K_2O$, (b) SiO_2, and (c) 1/Sr for the Cenozoic rocks of Vietnam. (1) Quartz tholeiite, (2) olivine tholeiite, (3) alkali basalt, and (4) xenoliths of granite and granodiorite.

the NHRL on the isotopic diagrams (Fig. 6), which is indicative of the influence of a source with Indian-Ocean isotopic signatures (I-MORB). It is noteworthy that an Indian-Ocean-type source was detected in both the ophiolite complexes of the basement of Pacific island arcs (Tu *et al.*, 1991, 1992) and the basalts of the late stages of marginal basin opening (Sumisu rift and Parece Vela basin) (Flower *et al.*, 2001). This allows us to infer that DUPAL-like asthenosphere probably existed there at least from the early Eocene (Flower *et al.*, 1998, 2001).

The problem of the nature of enrichment is the most complex and controversial. The similarity between the isotope geochemical characteristics of the enriched tholeiites and alkali basalts of the southeastern Asian margin and volcanics from a number of Pacific Ocean islands in the SOPITA region (Staudigel *et al.*, 1991) leads to the suggestion that there is a connection between the intraplate volcanism of the region and the activity of hot spots controlled by the lateral outflow of a lower mantle plume (Muruyama, 1994). A sub-Asian cratonic material delaminated and injected by asthenospheric components was considered as an alternative source for intraplate basalts (Mahoney *et al.*, 1992; Flower *et al.*, 2001).

The positive correlation between $^{87}Sr/^{86}Sr$ and $^{206}Pb/^{204}Pb$ in the basalts (Fig. 5) and the negative correlation between $^{143}Nd/^{144}Nd$ and $^{208}Pb/^{204}Pb$ imply a significant role of mixing between a moderately depleted asthenospheric source (I-MORB component) and an enriched EMII source (Tu *et al.*, 1992; Chung *et al.*, 1994, 1995; Zou *et al.*, 2000; etc.).

Another important feature of the basalts of southeastern China is the northward increase in $^{143}Nd/^{144}Nd$ and decrease in $^{87}Sr/^{86}Sr$ (Zou *et al.*, 2000) and $^{206}Pb/^{204}Pb$ (Chung *et al.*, 1994). The basalts of the northern part of the region (Nushan, Fangshan, and Tashan areas; Fig. 1) with the most depleted Sr–Nd ratios could reflect the isotopic composition of the asthenosphere, and the presence of DUPAL signatures suggests the existence of this anomaly in the asthenosphere before the processes of mixing with the EMII component (Zou *et al.*, 2000). Furthermore, the finding of xenoliths of depleted peridotites implied the existence of fragments of older lithosphere in this part of the region (Xu *et al.*, 2000). The isotopic similarity between the basalts of mainland China and the South China Sea suggests a resemblance of their mantle sources (Tu *et al.*, 1992; Chung *et al.*, 1994). It should be pointed out that the enriched isotopic and geochemical characteristics of basaltoids from the southern China region could in part be inherited from the subcontinental lithosphere (Chung and Sun, 1992; Tu *et al.*, 1992). It is known (e.g., Zindler *et al.*, 1984) that seamount basalts usually show sympathetic variations in geochemical and isotopic parameters. For instance, the basalts of the Scarborough seamounts are enriched in incompatible elements and have lower $^{143}Nd/^{144}Nd$ and higher $^{87}Sr/^{86}Sr$ and $^{206}Pb/^{204}Pb$ ratios. In contrast, the tholeiites of the outer zone of the Fujian province have lower $^{143}Nd/^{144}Nd$ and higher $^{87}Sr/^{86}Sr$ and $^{206}Pb/^{204}Pb$ ratios than the incompatible element enriched basaltoids of the inner zone, which probably reflects different contributions of either subcontinental lithosphere or deep plume material.

It is thought (e.g., Menzies *et al.*, 1980) that intraplate metasomatic and suprasubduction processes are the major factors of modification of the continental lithosphere from the moment of its formation. Extensive studies of the chemistry of deep xenoliths from the alkali basalts of the southern China and Indochina regions revealed varying degrees of metasomatic alter-

ation in the subcontinental lithosphere (Koloskov, 1999; Zhang and Cong, 1987; etc.).

Hydrous phases, such as amphibole and phlogopite, were found in the interstices of some lherzolites and as veinlets in composite xenoliths (Koloskov, 1999; Zhang and Cong, 1987; Tatsumoto *et al.*, 1992). The lherzolites characterize mainly a depleted source with low $^{87}Sr/^{86}Sr$ and high $^{143}Nd/^{144}Nd$ values. Enriched neodymium isotopic characteristics with an εNd of –1 were occasionally reported. The lead isotopic compositions of many xenoliths tend toward the EMII reservoir plotting above the NHRL. In addition, the isotopic composition of garnet lherzolite xenoliths from the basalts of the inner Fujian zone exhibits considerable variations in $^{87}Sr/^{86}Sr$ accompanied by a narrow $^{143}Nd/^{144}Nd$ range (Zhou and O'Nions, 1986; Tatsumoto *et al.*, 1992). The Sr–Nd isotopic characteristics of these rocks are similar to those of the host basalts, which can be regarded as evidence for metasomatic processes in the lithosphere beneath Southeast Asia. The metasomatic components could be related to either ancient subduction processes or intraplate plume-related magmatic events (EMI and EMII). Another possible mechanism for the formation of metasomatic components is connected with Mesozoic subduction beneath the southern China continental margin (Chung *et al.*, 1994). Although the convective transfer of the DUPAL isotopic anomaly from the southern hemisphere is theoretically possible (Hickey-Vargas, 1995), it is believed (Chung and Sun, 1992) that this ancient component could also be formed during the destruction of the continental cratonic lithosphere in response to the opening of the South China Sea.

Despite the geochemical similarity between the intraplate basaltoids of the south China and Indochina regions, there are certain differences in their isotopic compositions reflecting the lateral heterogeneity of mantle sources in Southeast Asia. It is noteworthy that, in contrast to the south China basaltoids, the basalts of Vietnam show an increase in the fraction of the enriched component EMI and a decrease in EMII at the transition from the quartz tholeiites of the early complex to the alkali basalts of the upper complex. This is generally consistent with changes from low-pressure melting conditions for quartz tholeiites to high-pressure for alkali basalts and with the heterogeneity of the mantle diapir.

The heterogeneity of the deep sources of the Vietnam basalts is most clearly seen in the isotopic mixing diagrams (Fig. 5b). According to the data of Hoang *et al.* (1996), the Nd and Sr isotopic compositions of the basalts changes from I-MORB-like to enriched OIB-like. Part of basalts with low $^{87}Sr/^{86}Sr$ and high $^{143}Nd/^{144}Nd$ ratios (Phuoc Long, Dalat, and Buon Ma Thuot) plot within the field of basalts from the South China Sea (Tu *et al.*, 1992) and Hainan Island (Tu *et al.*, 1991), whereas others (Dien Bien Phu, Quang Ngai/Re, Xuan Loc, Pleiku, and Song Cau) are shifted toward the field of enriched compositions and straddle the mixing line between the depleted mantle and the EMII end-member (Fig. 5a). In the Pb isotopic diagrams (Fig. 6), the basalts plot above the NHRL (Hart, 1988) forming approximately parallel trends between the compositions with high and low $^{206}Pb/^{204}Pb$ values. The basanites of Xuan Loc show the lowest $^{206}Pb/^{204}Pb$ values, and the basalts of other areas are more enriched (Hoang *et al.*, 1996).

The basalts of the first group from the Khorat Plateau show moderately depleted Nd–Sr–Pb isotopic characteristics corresponding to an I-MORB-type source but have high concentrations of HFSE and high Th/Yb and Ta/Yb ratios, which are indicative of their relation to a relatively enriched source (Zhou and Mukasa, 1997). Variations in the distribution of major and trace elements are mostly related to changes in the depth of magma formation and degree of mantle melting. The basalts of the Central Thai graben (Bo Phloi, Denchai, Chanthaburi, and Tha Mae areas) are chemically similar to the basalts of the first group from the Khorat Plateau. They also show no correlation between the silica or magnesium content, on the one hand, and isotopic composition, on the other hand, which is typical of crustal contamination processes. Characteristic features are the lack of influence of the enriched EMI component, which was observed in the lavas of eastern China (Tatsumoto *et al.*, 1992), and a minor contribution from the EMII component, which is related, according to Mukasa *et al.* (1996), to a subduction component (Fig. 5). The similarity of the chemical and isotopic compositions of the basalts of the first group from the Khorat Plateau and the Central Thai graben with the compositions of volcanics from southeastern China (Hainan Island and postspreading seamounts of the South China Sea) suggests the common nature of magma sources in these regions connected with the enriched mantle (Zhou and Mukasa, 1997).

Along with the resemblance to the basalts of the first group with respect to REE distribution, the basalts of the second group from the Khorat Plateau are distinguished by generally lower concentrations of highly incompatible elements. The isotopic characteristics of these basalts allow us to suppose their connection to an asthenospheric source contaminated with lithospheric material. In the Nd, Sr, and Pb isotopic diagrams, their compositions lie along the mixing curves between the components corresponding to moderately depleted I-MORB and EMII (Figs. 5, 6). Based on the absence of negative anomalies in HFSE distribution patterns, Zhou and Mukasa (1997) refuted the upper crustal pedigree of the EMII component and proposed a deeper source of contamination.

CONCLUSIONS

(1) Within southeastern Asia (southeastern China, Indochina, and adjoining marginal seas) several extensional-setting volcanic complexes of various ages were

distinguished: Early Tertiary, Miocene, Pliocene–Quaternary, and Quaternary. The Early Tertiary complex is formed by tholeiitic series volcanics, among which basalt–trachyte and basalt–basaltic andesite associations were recognized, and alkaline (mainly potassic) series basaltoids. The Miocene, Pliocene–Quaternary, and Quaternary complexes are dominated by tholeiitic and alkaline series basalts.

(2) The Early Tertiary basalt–trachyte and basalt–basaltic andesite associations of southeastern China show strong lateral chemical heterogeneity. The basalts and basaltic andesites of the Heyuan and Lienping grabens have moderately low HFSE and variable elevated LILE contents, high $^{87}Sr/^{86}Sr$, and low $^{143}Nd/^{144}Nd$, which, together with the negative correlation of $^{143}Nd/^{144}Nd$ and the positive correlation of $^{87}Sr/^{86}Sr$ with the concentrations of silica and LILE, suggests a considerable influence of crustal material on the petrogenesis of these volcanics. The volcanics of the Sanshui area are represented by the bimodal tholeiite–trachyte association, the basic members of which have moderately high HFSE and LILE concentrations and the trachytes are strongly enriched. The low-titanium potassic basaltoids (cocites and absarokites) of China and Vietnam are distinguished by LILE enrichment relative to HFSE, distinct negative Ta–Nb anomalies, and low Nb/U and Ce/Pb ratios.

(3) Most of the Miocene and Late Cenozoic volcanic centers of southeastern China and Indochina are composed of two eruptive complexes: (I) early high-silica, low-iron, and low-titanium quartz and olivine tholeiites and occasional trachyandesites characterizing the lithospheric type of mantle sources and (II) late low-silica, high-iron, and high-titanium olivine tholeiites, alkali basalts, basanites, and occasional trachybasalts and trachytes associated with an asthenospheric source.

The enriched tholeiites are compositionally similar to OIB and have differentiated REE distribution patterns. The transition from the quartz tholeiites to alkali basalts is accompanied by an increase in La/Hf, Ta/Yb, Zr/Y, Ba/Sr, Th/Yb, and La_n/Yb_n and a decrease in Hf/Ta, Zr/Nb, K_2O/P_2O_5, and Ti/Zr. The isotopic results for the tholeiites showed that their signatures changed from weakly depleted to moderately enriched relative to the BSE.

The Pleistocene–Holocene volcanics of the Okinawa Trough form a bimodal tholeiitic basalt–rhyolite series. Its main members are characterized by relatively high concentrations of incompatible elements similar to those of back-arc basin basalts and OIB (PREMA)-like Sr and Nd isotopic characteristics, but differ in a strong negative Ta–Nb anomaly and element ratios approaching the values of suprasubduction volcanics.

The basaltoids of the alkaline series have moderately high concentrations of alkalis, high titanium and phosphorus and low aluminum contents. Their incompatible element abundances are high and approach those of intraplate alkali basalts (OIB). The alkali basalts usually show a small positive Ta–Nb anomaly.

(4) The isotopic compositions of basalts from southeastern China, Indochina, and the adjoining marginal seas are in general controlled by the mixing between the DM and EMII components with a minor contribution from the EMI component, which was detected in some late alkaline basaltoid complexes (Flower *et al.*, 1998; Hoang *et al.*, 1996; Mukasa *et al.*, 1996).

The elevated (compared with the basalts of the Pacific Ocean) values of $^{207}Pb/^{204}Pb$ and $^{208}Pb/^{204}Pb$ (at given $^{206}Pb/^{204}Pb$) in the basalts led to the conclusion that an Indian-type asthenosphere (I-MORB or DUPAL-like) developed beneath the southeastern margin of the Eurasian continent (Flower *et al.*, 1998; Tu *et al.*, 1991; etc.).

REFERENCES

1. J. Angelier, F. Bergerat, H.-T. Chu, *et al.*, "Tectonic Analysis and the Evolution of a Curved Collision Belt: The Hsuenshan Range, Northern Taiwan," Tectonophysics **183**, 77–96 (1990).
2. S. M. Barr and A. S. Macdonald, "Geochemistry and Geochronology of Late Cenozoic Basalts of Southeast Asia," Geol. Soc. Am. Bull. (Part II) **92**, 1069–1142 (1981).
3. M. Barton and D. L. Hamilton, "Water-Undersaturated Melting Experiments Bearing upon the Origin of Potassium-Rich Magma," Mineral. Mag. **45**, 267–278 (1982).
4. A. R. Basu, J.-W. Wang, W.-K. Huang, *et al.*, "Major Element, REE, and Pb, Nd and Sr Isotopic Geochemistry of Cenozoic Volcanic Rocks of Eastern China: Implications for Their Origin from Suboceanic-Type Mantle Reservoirs," Earth Planet. Sci. Lett. **105**, 149–169 (1991).
5. O. A. Bogatikov, I. D. Ryabchikov, V. A. Kononova, *et al.*, *Lamproites* (Nauka, Moscow, 1991) [in Russian].
6. A. Briais, P. Tapponnier, and G. Pautot, "Constraints of Sea Beam Data on Crustal Fabrics and Sea Floor Spreading in the South China Sea," Earth Planet. Sci. Lett. **95**, 307–320 (1989).
7. S.-L. Chung and S.-S. Sun, "A New Genetic Model for the East Taiwan Ophiolite and Its Implications for Dupal Domains in the Northern Hemisphere," Earth Planet. Sci. Lett. **109**, 133–145 (1992).
8. S.-L. Chung, H. Cheng, B.-M. Jahn, *et al.*, "Major and Trace Element, and Sr–Nd Isotope Constraints on the Origin of Paleogene Volcanism in South China Prior to the South China Sea Opening," Lithos **40**, 203–220 (1997).
9. S.-L. Chung, B.-M. Jahn, S.-J. Chen, *et al.*, "Miocene Basalts in Northwestern Taiwan: Evidence for EM-Type Mantle Sources in the Continental Lithosphere," Geochim. Cosmochim. Acta **59**, 549–555 (1995).
10. S.-L. Chung, S.-S. Sun, K. Tu, *et al.*, "Late Cenozoic Basaltic Volcanism around the Taiwan Strait, SE China: Product of Lithosphere–Asthenosphere Interaction during Continental Extension," Chem. Geol. **112**, 1–20 (1994).

11. D. J. DePaolo, *Neodymium Isotope Chemistry: An Introduction* (Springer-Verlag, New York, 1988).
12. A. E. Dovzhikov, Bui Fu Mi, E. D. Vasilevskaya, *et al.*, *The Geology of Northern Vietnam* (Hanoi, 1965) [in Russian].
13. J. Encarnacion, D. Fernandez, and J. Mattinson, "Subduction Initiation by Extrusion Tectonics? Evidence from the Palawan Ophiolite, Philippines," EOS Trans. AGU Fall Meet. **82**, 302 (2001).
14. Q. Fan and P. R. Hooper, "The Cenozoic Basaltic Rocks of Eastern China: Petrology and Chemical Composition," J. Petrol. **32**, 765–810 (1991).
15. P. I. Fedorov and N. I. Filatova, "Geochemistry and Petrology of Late Cretaceous and Cenozoic Basalts from Extensional Zones at the Continental Margin of Northeastern Asia," Geokhimiya, No. 2, 115–132 (1999) [Geochem. Int. **37**, 91–107 (1999)].
16. P. I. Fedorov and N. I. Filatova, "Cenozoic Volcanism of Korea," Geokhimiya, No. 1, 3–29 (2002) [Geochem. Int. **40**, 1–25 (2002)].
17. P. I. Fedorov, A. V. Koloskov, and S. M. Lyapunov, "Geochemistry and Petrology of Late Cenozoic Volcanics from the Navarin Foreland, East Koryak Highlands," Geokhimiya, No. 9, 1284–1296 (1993).
18. N. I. Filatova and P. I. Fedorov, "Cenozoic Magmatism of Extension Zones in Continental Margins: An Example of the Korea–Japan Area," Petrologiya **9**, 519–546 (2001) [Petrology **9**, 450–476 (2001)].
19. M. F. J. Flower, M. Zhang, C.-Y. Chen, *et al.*, "Magmatism in the South China Basin: 2. Post-Spreading Quaternary Basalts from Hainan Island, South China," Chem. Geol. **97**, 65–87 (1992).
20. M. F. J. Flower, K. Tamaki, and N. Hoang, "Mantle Extrusion: A Model for Dispersed Volcanism and DUPAL-Like Asthenosphere in East Asia and the Western Pacific," in *Mantle Dynamics and Plate Interactions in East Asia*, Ed. by M. F. J. Flower, S.-L. Chung, C.-H. Lo, and T.-Y. Lee (AGU, Washington, 1998), pp. 67–88.
21. M. F. J. Flower, R. M. Russo, K. Tamaki, and N. Hoang, "Mantle Contamination and the Izu–Bonin–Mariana (IBM) 'High-Tide Mark': Evidence for Mantle Extrusion Caused by Tethyan Closure," Tectonophysics **333**, 9–34 (2001).
22. S. R. Hart, "Heterogeneous Mantle Domains: Signatures, Genesis and Mixing Chronologies," Earth Planet. Sci. Lett. **90**, 273–296 (1988).
23. W. K. Hart, G. G. Wolde, R. C. Walter, *et al.*, "Basaltic Volcanism in Ethiopia: Constraints on Continental Rifting and Mantle Interactions," J. Geophys. Res. **94**, 7731–7748 (1989).
24. R. Hickey-Vargas, J. M. Herget, and P. Spadea, The Indian Ocean-Type Isotopic Signature in Western Pacific Marginal Basins: Origin and Significance," in *Active Margins and Marginal Basins of the Western Pacific* (AGU, Washington, 1995), pp. 175–198.
25. T. T. Hoa, N. T. Yem, N. T. Phuong, *et al.*, "Magnesian–Ultrapotassic Magmatic Rocks and Lamproite Problems in Northwestern Vietnam," in *Proceedings of IGCP Symposium on the Geology of SE Asia, Hanoi, November 1995*, J. Geol. Ser. B., Nos. 5–6, 412–419 (1995).
26. N. Hoang and M. F. J. Flower, "Petrogenesis of Cenozoic Basalts from Vietnam: Implication for Origins of a 'Diffuse Igneous Province'," J. Petrol. **39**, 369–395 (1998).
27. N. Hoang, M. F. J. Flower, and R.W. Carlson, "Major, Trace Elements, and Isotopic Compositions of Vietnamese Basalts: Interaction of Hydrous EMI-Rich Asthenosphere with Thinned Eurasian Lithosphere," Geochim. Cosmochim. Acta **60**, 4329–4351 (1996).
28. B. M. Jahn, "Mid-Ocean Ridge or Marginal Basin Origin of the East Taiwan Ophiolite: Chemical and Isotopic Evidence," Contrib. Mineral. Petrol. **92**, 194–206 (1986).
29. V. E. Khain, *Tectonics of Continents and Oceans in 2000* (Nauchnyi Mir, Moscow, 2001) [in Russian].
30. M. Kimura, "Back-Arc Rifting in the Okinawa Trough," Mar. Petrol. Geol. **2**, 222–240 (1985).
31. A. V. Koloskov, *Ultrabasic Inclusions and Volcanics as a Self-Regulated Geologic System* (Nauchnyi Mir, Moscow, 1999) [in Russian].
32. A. V. Koloskov, G. B. Flerov, and A. Ya. Sharas'kin, "Rift-Related Volcanism in the System of Eastern Asian Volcanic Belts," in *Magmatism of Rifts: Petrology, Evolution, Geodynamics*, Ed. by O. A. Bogatikov (Nauka, Moscow, 1989), pp. 139–144 [in Russian].
33. A. V. Koloskov, V. A. Rashidov, Yu. G. Gatinskii, *et al.*, "Late Cenozoic Volcanism in the Continental and Shelf Zones of Vietnam," in *Proceedings of the Annual Conference Devoted to the Day of Volcanologists* (Nauka dlya Kamchatki, Petropavlovsk-Kamchatskii, 2003), pp. 9–15 [in Russian].
34. H. R. Kudrass, M. Wiedicke, P. Cepek, *et al.*, "Mesozoic and Cenozoic Rocks Dredged from the South China Sea (Reed Bank Area) and Sulu Sea, and Their Significance for Plate Tectonic Reconstruction," Mar. Petrol. Geol. **3**, 19–30 (1986).
35. Kung-Suan Ho, J.-C. Chen, and W.-S. Juang, "Geochronology and Geochemistry of Late Cenozoic Basalts from the Leiqiong Area, Southern China," J. Asian Earth Sci. **18**, 307–324 (2000).
36. *Large Igneous Provinces*, Ed. by J. Mahoney and M. F. Coffin (AGU, Washington, 1997).
37. T.-Y. Lee, C.-Y. Chen, C.-H. Lo, *et al.*, "Preliminary Results of ^{40}Ar–^{39}Ar Dating of Cenozoic Basalts in the Indochina Region and Its Tectonic Implications," J. Asian Earth Sci. **94**, 117–128 (1998).
38. X. Le Pichon, M. Fournier, and L. Jolivet, "Kinematics, Topography, Shortening, and Extrusion in the India–Eurasia Collision," Tectonics **11**, 1085–1098 (1992).
39. M. Loubet, R. Sassi, and G. DiDonato, "Mantle Heterogeneities: A Combined Isotope and Trace Element Approach and Evidence for Recycled Continental Crust Materials in Some OIB Sources," Earth Planet. Sci. Lett. **89**, 299–315 (1988).
40. J. J. Mahoney, A. P. LeRoex, Z. Peng, *et al.*, "Southwestern Limits of Indian Ocean Ridge Mantle and the Origin of Low-$^{206}Pb/^{204}Pb$ Mid-Ocean Ridge Basalts: Isotope Systematics of the Central Southwest Indian Ridge (17°–50° E)," J. Geophys. Res. **97**, 19771–19790 (1992).
41. S. Maruyama, "Plume Tectonics," J. Geol. Soc. Japan **100**, 24–49 (1994).
42. M. A. Menzies and V. R. Murthy, "Nd and Sr Isotope Geochemistry of Hydrous Mantle Nodules and Their Host Alkali Basalts: Implications for Local Heterogene-

ities in Metasomatically Veined Mantle," Earth Planet. Sci. Lett. **46**, 323–334 (1980).

43. E. E. Milanovskii and A. M. Nikishin, "West Pacific Rift Belt," Byull. Mosk. O–va Ispyt. Prir., Otd. Geol. **63** (4), 3–15 (1988).
44. S. B. Mukasa, G. M. Fischer, and S. M. Barr, "The Character of the Subcontinental Mantle in Southeast Asia: Evidence from Isotopic and Elemental Compositions of Extension-Related Cenozoic Basalts in Thailand," in *Earth Processes: Reading Isotopic Code* (AGU, Washington, 1996), pp. 233–252.
45. V. M. Novikov, V. V. Ivanenko, M. I. Karpenko, and A. V. Koloskov, "Age of Young Volcanism in Southeastern Indochina," Izv. Akad. Nauk SSSR, Ser. Geol., No. 6, 39–44 (1989).
46. Z. C. Peng, R. E. Zartman, K. Futa, *et al.*, "Pb-, Sr- and Nd-Isotopic Systematics and Chemical Characteristics of Cenozoic Basalts, Eastern China," Chem. Geol. **59**, 3–33 (1986).
47. G. V. Polyakov, N. Ch. Iem, P. A. Balykin, *et al.*, "New Data on Ultrapotassic Basic Rocks of Northern Vietnam, Cocites," Geol. Geofiz. **38**, 148–158 (1997).
48. C. Rangin, M. Klein, D. Rogues, *et al.*, "The Red River Fault System in the Tonkin Gulf, Vietnam," Tectonophysics **243**, 209–222 (1995).
49. S. V. Rasskazov, N. A. Logachev, I. S. Brandt, *et al.*, *Geochronology and Geodynamics of the Late Cenozoic in Southern Siberia, Southern and Eastern Asia* (Nauka, Novosibirsk, 2000) [in Russian].
50. R. Shinjo and Y. Kato, "Geochemical Constraints on the Origin of Bimodal Magmatism at the Okinawa Trough, and Incipient Back-Arc Basin," Lithos **54**, 117–137 (2000).
51. R. Shinjo, S.-L. Chung, Y. Kato, *et al.*, "Geochemical and Sr–Nd Isotopic Characteristics of Volcanic Rocks from the Okinawa Trough and Ryukyu Arc: Implications for the Evolution of a Young, Intracontinental Back-Arc Basin," J. Geophys. Res. **104**, 10591–10608 (1999).
52. H. Staudigel, K.-H. Park, M. Pringle, *et al.*, "The Longevity of the South Pacific Isotopic and Thermal Anomaly," Earth Planet. Sci. Lett. **102**, 24–44 (1991).
53. S.-S. Sun and W. F. McDonough, "Chemical and Isotopic Systematics of Oceanic Basalts," in *Magmatism in Ocean Basins*, Ed. by A. D. Saunders and M. J. Norry, Geol. Soc. Spec. Publ. **42**, 313–345 (1989).
54. W. H. Sun and Z. M. Lai, "Petrochemical Characteristics of Cenozoic Volcanic Rocks in Fujian Province and Its Relationship to Tectonics," Geochimica **1**, 134–147 (1980).
55. P. Tapponnier, G. Peltzer, and R. Armijo, "On the Mechanics of the Collision between India and Asia," in *Collision Tectonics*, Ed. by M. R. Coward and A. C. Ries, Geol. Soc. Spec. Publ. **19**, 115–157 (1986).
56. M. Tatsumoto, A. R. Basu, H. Wankang, *et al.*, "Sr, Nd, and Pb Isotopes of Ultramafic Xenoliths in Volcanic Rocks of Eastern China: Enriched Components EMI and EMII in Subcontinental Lithosphere," Earth Planet. Sci. Lett. **113**, 107–128 (1992).
57. B. Taylor and D. E. Hayes, "Origin and History of the South China Basin," in *The Tectonic and Geologic Evolution of Southeast Asian Seas and Islands* (AGU, Washington, 1983), pp. 25–56.
58. K. Tu, M. F. J. Flower, R. W. Carlson, *et al.*, "Sr, Nd, and Pb Isotopic Compositions of Hainan Basalts (South China): Implications for a Subcontinental Lithosphere Dupal Source," Geology **19**, 567–569 (1991).
59. K. Tu, M. F. J. Flower, R. W. Carlson, *et al.*, "Magmatism in the South China Basin 1. Isotopic and Trace-Element Evidence for an Endogenous Dupal Mantle Component," Chem. Geol. **97**, 47–63 (1992).
60. N. X. Tung and T. V. Tri, *Structural Map of Vietnam, 1 : 1000000* (Geol. Surv. Vietnam, Hanoi, 1992).
61. S. Turner, N. Arnaud, J. Liu, *et al.*, "Post-Collision, Shoshonitic Volcanism on the Tibetan Plateau: Implications for Convective Thinning of the Lithosphere and the Source of Ocean Island Basalts," J. Petrol. **37**, 45–71 (1996).
62. M. Wang, D. Wu, I. Liang, *et al.*, "Some Geochemical Characteristics of Basalts from the South China Sea," Geochimica **4**, 332–340 (1986).
63. J. L. Whitford-Stark, "A Survey of Cenozoic Volcanism on Mainland Asia," Geol. Soc. Spec. Publ. **213** (1987).
64. D. A. Wood, "The Application of a Th–Hf–Ta Diagram to Problems of Tectonomagmatic Classification and to Establishing the Nature of Crustal Contamination of Basaltic Lavas of the British Tertiary Volcanic Province," Earth Planet. Sci. Lett. **50**, 11–30 (1980).
65. X. Xu, S. Y. O'Reilly, and W. L. Griffin, "Genesis of Young Lithospheric Mantle in Southeastern China: An ICPMS Trace Element Study," J. Petrol. **41**, 111–148 (2000).
66. V. V. Yarmolyuk, V. S. Samoilov, V. G. Ivanov, *et al.*, "Composition and Sources of Basalts in the Late Paleozoic Rift System of Central Asia: Geochemical and Isotopic Data," Geokhimiya, No. 10, 1027–1042 (1999) [Geochem. Int. **37**, 921–935 (1999)].
67. R. Y. Zhang and B. L. Cong, "The Cenozoic Volcanic Rocks and Their Bearing Ultramafic Xenoliths in South China," in *Cenozoic Basaltic and Mantle-Derived Xenoliths in Eastern China*, Ed. by M. L. Eh (Sci. Press, Beijing, 1987), pp. 349–475.
68. P. Zhou and S. B. Mukasa, "Nd–Sr–Pb Isotopic and Major- and Trace-Element Geochemistry of Cenozoic Lavas from the Khorat Plateau, Thailand: Sources and Petrogenesis," Chem. Geol. **137**, 175–193 (1997).
69. X. Zhou and R. K. O'Nions, "Pb–Nd–Sr Systematics of Xenoliths from East China," Terra Cognita **6**, 244 (1986).
70. B. Q. Zhu, Y. Q. Zhang, and Y. W. Xie, "Nd, Sr, and Pb Isotope Characteristics of Cenozoic Ultrapotassic Volcanic Rocks from Haidong, Yunnan, and Their Implications for Subcontinental Mantle Evolution in Southwestern China," Geochimica **21**, 201–212 (1992).
71. A. Zindler and S. Hart, "Chemical Geodynamics," Annu. Rev. Earth Planet. Sci. **14**, 493–571 (1986).
72. A. Zindler, H. Staudigel, and R. Batiza, "Isotope and Trace Geochemistry of Young Pacific Seamounts: Implications for the Scale of Upper Mantle Heterogeneity," Earth Planet. Sci. Lett. **70**, 175–195 (1984).
73. H. Zou, A. Zindler, X. Xu, *et al.*, "Major, Trace Element, and Nd, Sr and Pb Isotope Studies of Cenozoic Basalts in SE China: Mantle Sources, Regional Variations, and Tectonic Significance," Chem. Geol. **171**, 33–47 (2000).